Special Report #157

FULL-SCALE TESTS OF 4- AND 6-BLADE, SINGLE- AND DUAL-ROTATING PROPELLERS

By David Biermann and Edwin P. Hartman
Langley Memorial Aeronautical Laboratory

August 1940

FULL-SCALE TESTS OF 4- AND 6-BLADE, SINGLE- AND DUAL-ROTATING PROPELLERS

By David Biermann and Edwin P. Hartman

SUMMARY

Tests of 10-foot diameter, 4- and 6-blade single- and dual-rotating propellers were conducted in the 20-foot propeller-research tunnel. The propellers were mounted at the front end of a streamline body incorporating spinners to house the hub portions. The effect of a symmetrical wing mounted in the slipstream was investigated. The blade angles investigated ranged from 20° to 65°; the latter setting corresponds to airplane speeds of over 500 miles per hour.

The results indicate that dual-rotating propellers were from 0 to 6 percent more efficient than single-rotating ones; but when operating in the presence of a wing the gain was reduced about one-half. Other advantages of dual-rotating propellers were found to include greater power absorption and greater efficiency at the low V/nD operating range of high pitch propellers.

INTRODUCTION

Theoretical treatments of propeller losses, such as those given in references 1 and 2, have indicated rotational losses in the slipstream amounting to several percent for highly loaded propellers operating at high values of V/nD. Military aircraft have now reached the stage of speed and power wherein it appears that dual-rotating propellers might be justified on the grounds of improved efficiency alone; although the elimination of the engine-torque reaction might be a more important consideration. In view of these advantages of dual-rotating propellers over single-rotating ones, the need for full-scale propeller tests is obvious, inasmuch as very little information on the subject is available.

A test program was initiated for the 20-foot propeller-research tunnel to cover the following conditions: Tests of 2-, 3-, 4-, 6-, and 8-blade single-rotating propellers operating both as tractors and pushers; tests of 4-, 6-, and 8-blade dual-rotating propellers operating

both as tractors and pushers; tests to determine the effect of a wing in reducing the slipstream rotational losses.

The present report covers the results of the tractor tests made with 2-, 3-, 4-, and 6-blade single- and 4- and 6-blade dual-rotating propellers operating with and without a wing in the slipstream.

APPARATUS AND METHODS

The tests were made in the NACA 20-foot propeller-research tunnel.

Propellers.- The propellers which incorporate the Clark Y section were approximately 10 feet in diameter. They varied slightly in diameter, depending on the hub used. The drawing numbers are Hamilton-Standard 3155-6 for the right-hand blades and Hamilton-Standard 3156-5 for the left-hand blades. Blade-form curves are given in figure 1.

Driving mechanism.- The propellers were driven by two 25-horsepower electric motors arranged in tandem. (See fig. 2.) The front motor was directly connected to the front propeller while the rear motor drove the rear propeller through chains and a countershaft. The propeller shafts were locked together for single-rotation operating conditions. The motors were mounted on bearings concentric with the shaft axis. Each motor frame was restrained from rotating by helical springs connecting with the supporting frame, which provided means for measuring the torque. Selsyn motors were used to transmit the motion of the motor frames to the test chamber in order that torque measurements could be made.

Body.- An outline of the streamline body housing the motors is shown in figure 3. A photograph of the set-up is given in figure 4. Tests were made with and without the symmetrical wing in place. The wing was located in the midwing position, and set at an angle of attack of 0°. Both ends of the body were made identical in order that comparative tractor and pusher tests could be made without altering the body shape. Spinners were used for all tests. Both wing and body were constructed of wood-forming members covered with sheet-aluminum skin.

Measurements.- The net thrust or drag of the propeller-body combination was measured on a thrust balance located on the floor of the test chamber. The torque of each motor

was measured with the spring-dynamometer-selsyn-repeating system described above. The dynamometer was calibrated before and after the series of tests was made. Friction-determination tests were made frequently during the program. The propeller speed was measured by a new NACA electric tachometer which proved to be highly accurate. The tachometer was frequently checked during runs against a tuning fork. Each propeller of the dual combinations was run at the same speed. A synchroscope was used to indicate synchronism. Control of the relative speeds of the two motors was obtained with a frequency converter placed in the line feeding one of the induction drive motors.

Test conditions.- The tunnel speed ranged from 0 to about 110 miles per hour. The maximum propeller speed was about 550 rpm, which corresponds to 287 feet per second rotational tip speed.

The dual-rotation tests were made with the rear propeller blades adjusted to provide approximately the same torque at peak efficiency as for the front propeller. A plot of the difference between the front and rear propeller-blade settings is given in figure 5. A typical plot of the results is given in figure 6. The degree that the test points scatter gives an indication of the accuracy of the results.

The 4- and 6-blade single-rotating propellers were made up with two 2- and 3-way hubs, respectively, mounted in tandem. Alternate blades were thus staggered. This arrangement resulted in identical blade shank and spinner conditions for both the single- and dual-rotation tests.

RESULTS AND DISCUSSION

The measured values have been reduced to the usual coefficients of thrust, power, and propulsive efficiency,

$$C_T = \frac{\text{effective thrust}}{\rho\, n^2\, D^4}$$

$$C_P = \frac{\text{engine power}}{\rho\, n^3\, D^5}$$

and

$$\eta = \frac{C_T}{C_P}\,\frac{V}{nD}$$

$$C_S = \sqrt[5]{\frac{\rho V^5}{P n^2}}$$

where the effective thrust is the measured thrust of the propeller-body combination plus the drag of the body measured separately.

D propeller diameter, feet.

n propeller rotational speed, rps.

These coefficients were plotted against V/nD. The results are given in the following figures:

Figure	Number of blades	Rotation	Wing
7 to 9	4	Single	No
10 to 13	4	Dual	No
14 to 16	6	Single	No
17 to 20	6	Dual	No
21 to 23	4	Single	Yes
24 to 27	4	Dual	Yes
28 to 30	6	Single	Yes
31 to 34	6	Dual	Yes
35 to 36	Effect of small variations in blade angles for dual propeller.		
37	Envelope efficiency comparisons.		
38 to 39	Comparisons of power absorbed.		
40	Comparisons of thrust available at constant power.		
41 to 44	Design C_s charts.		

In addition to the comparisons listed above, several direct comparisons are made between the 6-blade single- and dual-propeller characteristics in figures 17 to 20 and 31 to 34.

The dual-rotation tests were conducted with the rear

propeller set at a slightly lower angle than the front one in order to absorb approximately the same power at the peak-efficiency condition. (See fig. 5 for blade settings.) The necessity for this difference in blade angle can be explained by the fact that the front propeller introduces a rotational component to the slipstream which increases the angle of attack of the rear propeller. It is then necessary to reduce the blade angle of the rear propeller to offset this increased angle of attack.

The front propeller also adds energy to the stream in the form of an increment of pressure across the propeller disk. The pressure energy is gradually converted into velocity energy as the flow progresses. For closely spaced dual-rotating propellers the velocity through the rear propeller disk is very little different from that through the front propeller disk, hence the blade-angle increment of the rear propeller necessary to offset this increased velocity is probably very little. If the propeller spacing were large the velocity factor would be quite perceptible and might even overbalance the rotational factor.

In figures 12, 19, 26, and 33, it may be noted that the power curves for the front and rear propellers cross at V/nD values corresponding approximately to those for peak efficiency, and that at lower V/nD values the rear propeller absorbs considerably more power than the front propeller. This illustrates further the effect of the front propeller in increasing the angle of attack of the rear propeller, and indicates that the magnitude of the differences in the power absorbed by the front and rear propellers is a direct function of the disk loading, as would be expected from theory.

In figures 35 and 36 are shown the results from a few tests made to determine the effect of small changes in the blade angle of the rear propeller. It may be noted that the thrust and power changed as would be expected, and that there was no measurable effect on the efficiency of the combination.

There are several important considerations in comparing single- and dual-rotating propellers. The relative efficiency at all speeds is obviously of the first order of importance. The presence of a wing in the slipstream is an important consideration because it can be expected to remove about half of the race rotation of a single propeller. The relative power absorbed at peak efficiency

by single- and dual-rotating propellers is of some importance because of its effect on the diameter and tip speed. The relative power absorbed at the take-off and climbing conditions determines the relative blade-angle settings and consequently the relative thrust. The relative thrust for a given power output is a measure of the relative efficiencies for the take-off and climb of controllable propellers.

In figure 37 are the envelope efficiency comparisons for all conditions investigated. The 4-blade dual-rotating propeller had about the same efficiency as the single-rotating propeller at a V/nD of about 1.0; but at a V/nD of 5.0 there was a gain of 5 percent in favor of dual rotation. The wing improved the efficiency of the single-rotating propeller about 2 percent only for the high V/nD range. The wing had no effect on the 4-blade dual-propeller results.

The 6-blade dual-rotation propeller was from 1 to 6 percent more efficient than the single-rotation propeller. The wing improved the efficiency of the single-rotation propeller by 0 to 4 percent, and also improved the efficiency of the dual propeller 0 to 3 percent.

These results seem to check theory roughly in that the gain due to dual rotation, within the limits of these tests, amounts to from 0 to about 6 percent, depending upon the pitch and the disk loading. The presence of the wing resulted in about half as much improvement in efficiency as dual rotation.

In figure 37 is also shown the effect of different numbers of blades on efficiency. The results for the 2- and 3-blade propellers, which are included here for comparison, are the average of the results of the tests made with the propellers located in the front and rear positions. Inasmuch as the rear spinner is larger than the front one, the efficiency of the rear propeller was found to be 1 or 2 percent higher than that of the front one. Using average results for the 2- and 3-blade propellers makes possible a direct comparison with the 4- and 6-blade propellers, each of which was made up with half of the blades located in the front and half in the rear position. It may be noted that there was very little difference between the efficiencies of the 2-, 3-, 4-, and 6-blade propellers, except for the low V/nD range. At high values of V/nD the 6-blade propeller was only about 2 percent

less efficient than the 3-blade one. It should be pointed out, however, that solidity comparisons of this type do not necessarily bring out the true significance, inasmuch as the disk loading was not the same for each propeller. A separate report covers this subject more thoroughly.

In figures 38 and 39 the relative power absorbed by single- and dual-rotating propellers is given for three flight conditions. The comparisons are made on the basis of the same effective blade angles, viz, the dual propeller results were interpolated to bring the V/nD for zero thrust in coincidence with that for the single propeller. The results indicate that the 4-blade single and dual propellers absorbed about the same power for the peak efficiency condition; but that at V/nD values corresponding to the take-off and climbing conditions the dual-rotating propeller absorbed 5 to 17 percent more power than the single propeller. The 6-blade comparison (fig. 39) shows more pronounced effects, even for the high-speed condition; the dual propeller absorbed several percent more power for the high-speed condition and as much as 30 percent more power for the take-off condition. This means that the diameter of the dual propeller will be smaller than that of the single one for equal power absorption, and that the blade angles for the take-off and climbing conditions will be lower.

The relative thrust available for dual and single propellers operating at equal values of C_p is given in figure 40. This is a true comparison of controllable propellers of equal diameters operating at all flight speeds but at constant torque, engine speed, and altitude; and consequently shows the direct effect of dual propellers on the thrust for the take-off and climbing conditions. Relative thrust curves are worked out for several airplane categories, defined by the blade-angle settings for high speed. Thus 30°, 45°, 50°, 55°, 60°, and 65° high speed settings correspond roughly to speeds of 250, 375, 425, 450, 475, 500, and 525 miles per hour, respectively, assuming a tip speed of 900 to 1000 feet per second. Inasmuch as the engine speed and diameter are assumed constant, the V/nD is directly proportional to the air speed.

This analysis indicates that there is a marked gain due to dual rotation for the take-off and climb of airplanes operating at conditions of C_p greater than 0.4, or for conditions wherein the blade angles for take-off

and climb exceed 30°. In terms of airplane categories, the take-off and climbing thrust of airplanes having high speeds at sea level in excess of about 375 miles per hour would be benefited by dual-rotating propellers. Airplanes having high speeds at 20,000 feet greater than about 460 miles per hour would have take-off blade angles (assuming equal power) in excess of 30° and consequently would benefit by dual rotation for this condition; the benefit would be even greater for the climbing condition at 20,000 feet.

An example calculation will illustrate this point.

Given: High speed of 500 miles per hour at 20,000 feet

β for high speed = 60°

V/nD for high speed = 3.6

C_P for high speed = 1.118

To find relative thrust at reduced speeds,

V/nD for climb at 20,000 feet = $3.6 \times 0.65 = 2.34$

C_{T_D}/C_{T_S} = 1.2 (climb at 20,000 feet)

C_P for sea level = 0.595 (assuming constant engine power)

C_{T_D}/C_{T_S} = 1.06 (climb at sea level)

V/nD for take-off = $0.35 \times 3.6 = 1.26$ (assuming constant engine speed)

C_{T_D}/C_{T_S} = 1.15

CONCLUSIONS

1. The peak efficiency of dual-rotating 4- and 6-blade tractor propellers was found to be from 0 to 6 percent greater than that of single-rotating ones, depending upon the disk loading and the blade-angle setting; the higher these values, the greater the difference in efficiency up to the limiting test blade angle of 65°.

2. The presence of a wing in the slipstream increased the efficiency of single-rotating propellers about half as much as was obtained with dual operation.

3. Dual-rotating propellers absorbed only slightly more power at peak efficiency than did single-rotating ones; but at V/nD values corresponding to the take-off and climbing conditions, the difference was more pronounced.

4. The take-off and climbing thrust of dual-rotating, controllable propellers for airplanes in the 400-miles-per-hour-and-up category were found to exceed that for single-rotating propellers by substantial margins.

Langley Memorial Aeronautical Laboratory,
National Advisory Committee for Aeronautics,
Langley Field, Va.

REFERENCES

1. Weinig, F.: Counter-Rotating Propellers for Aircraft. Jahrbuch der deutschen Luftfahrtforschung, 1937.

2. Lazzarino, Lucio: Study of Airscrews for High Speed Aeroplanes. Jour. R.A.S., April 1940.

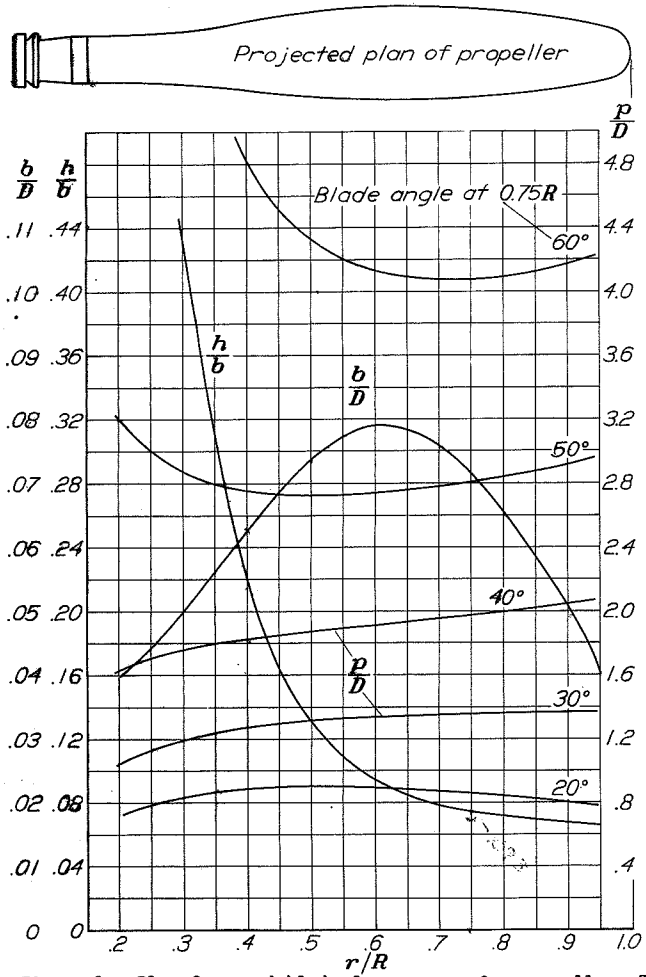

Figure 1.- Plan-form and blade-form curves for propellers 3155-6 and 3156-6. D, diameter; R, radius to the tip; r, station radius; b, section chord; h, section thickness; p, geometric pitch.

AF - 90

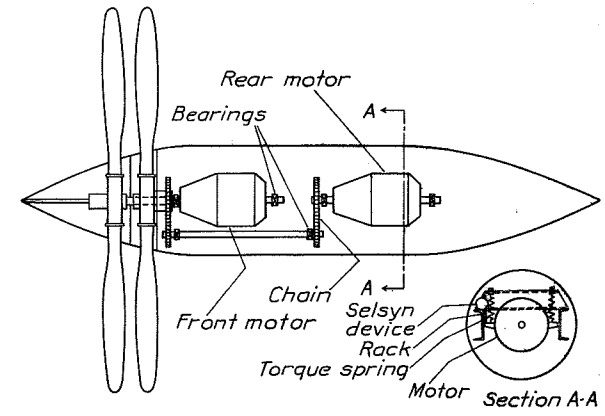

Figure 2.- Propeller drive mechanism.

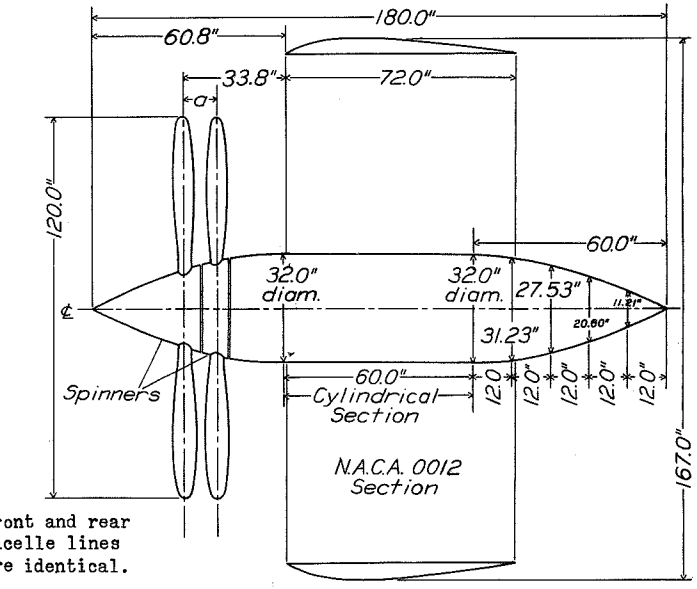

Note: Front and rear nacelle lines are identical.

Figure 3.- Plan view showing dimensional details of wing and nacelle. Dimension a for four-blade propeller = 9.7" and for six-blade propeller = 10.0".

NACA

Figs. 1,2,3.

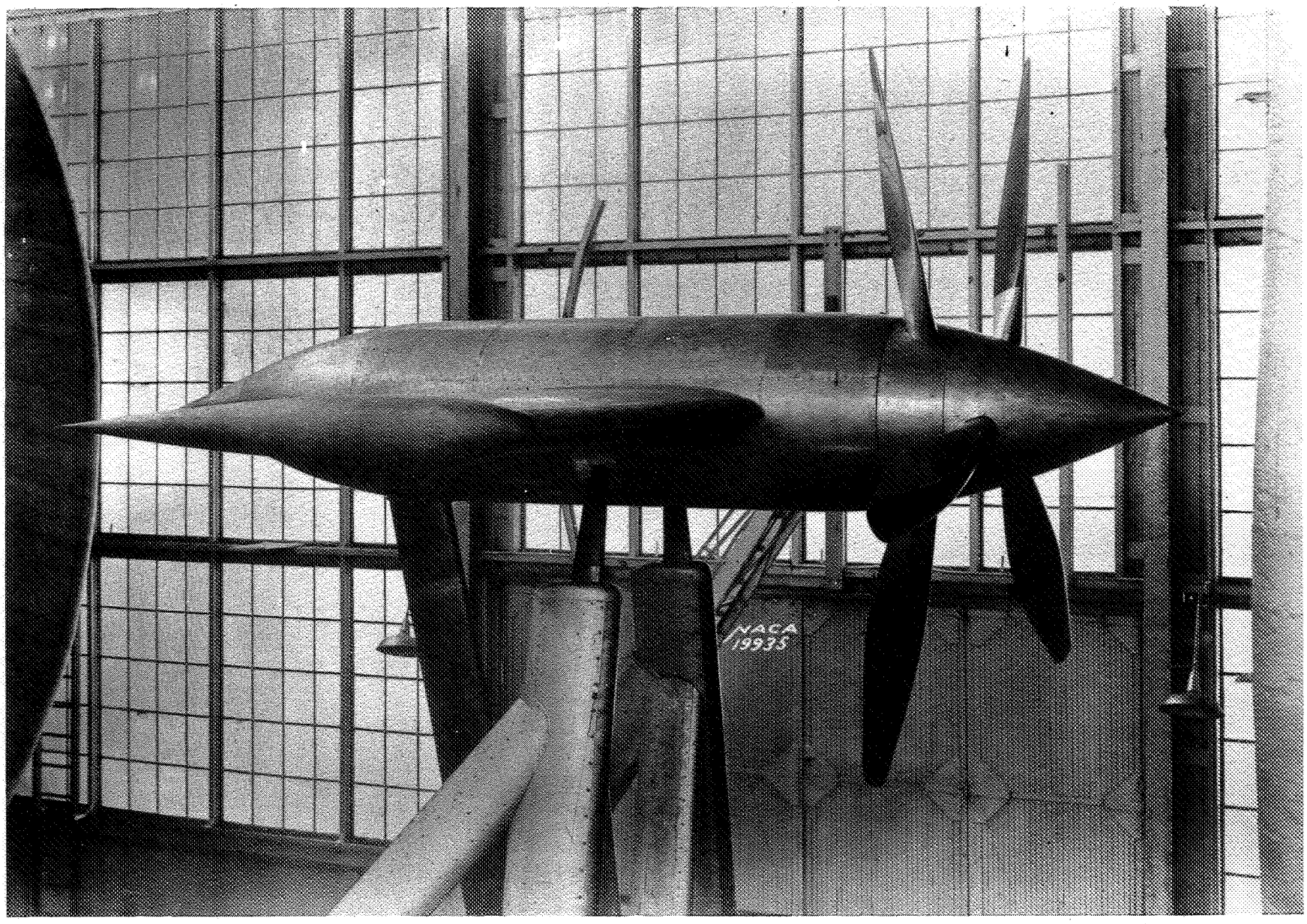

Figure 4.- Test set-up. The photograph shows a six-blade single-rotation propeller with wing in place.

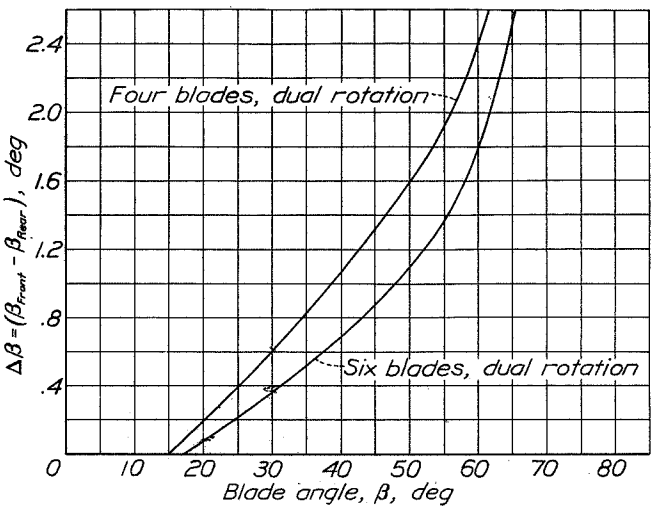

Figure 5.- Difference in blade angle for equal torque at peak efficiency.

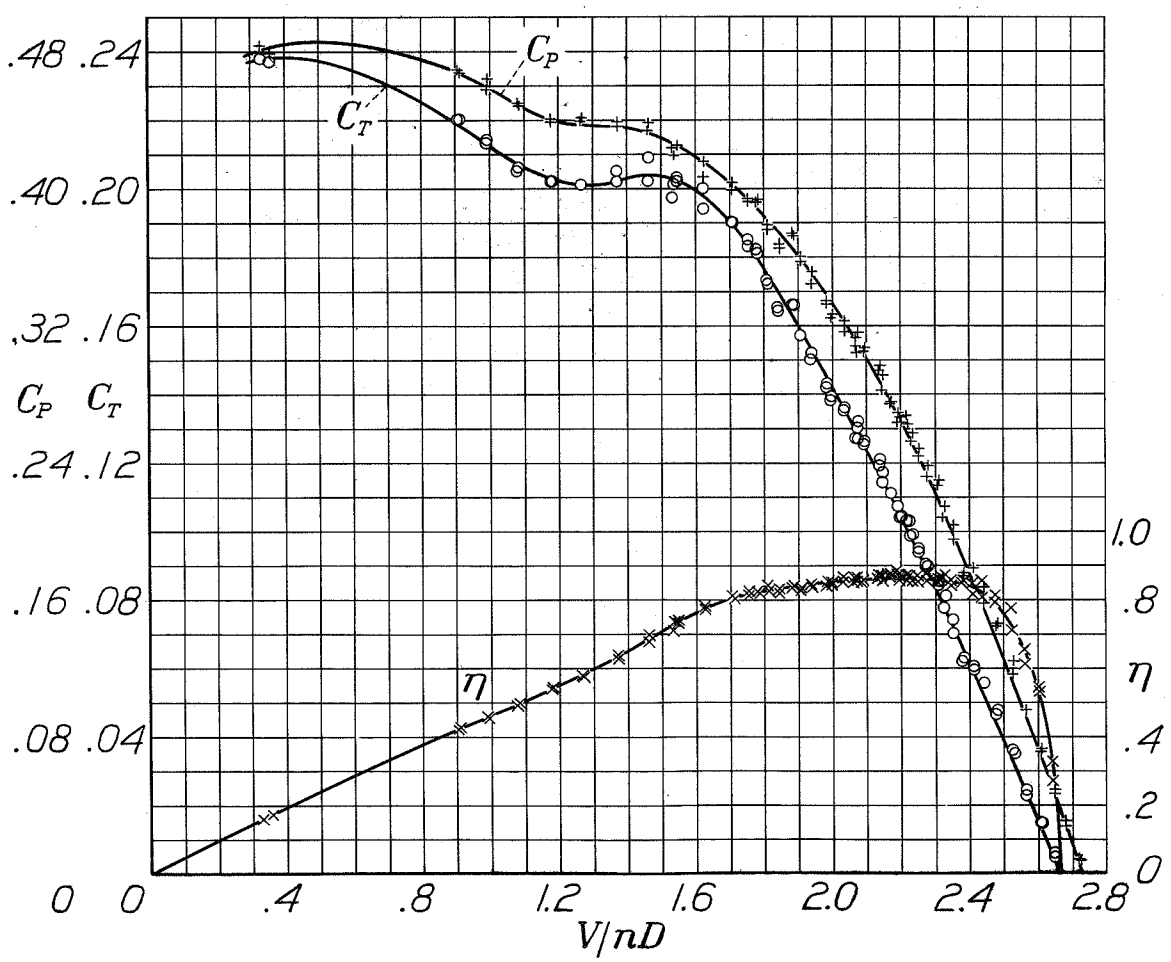

Figure 6.- Typical test results. Four-blade single-rotation with wing. Propeller set 45° at 0.75R.

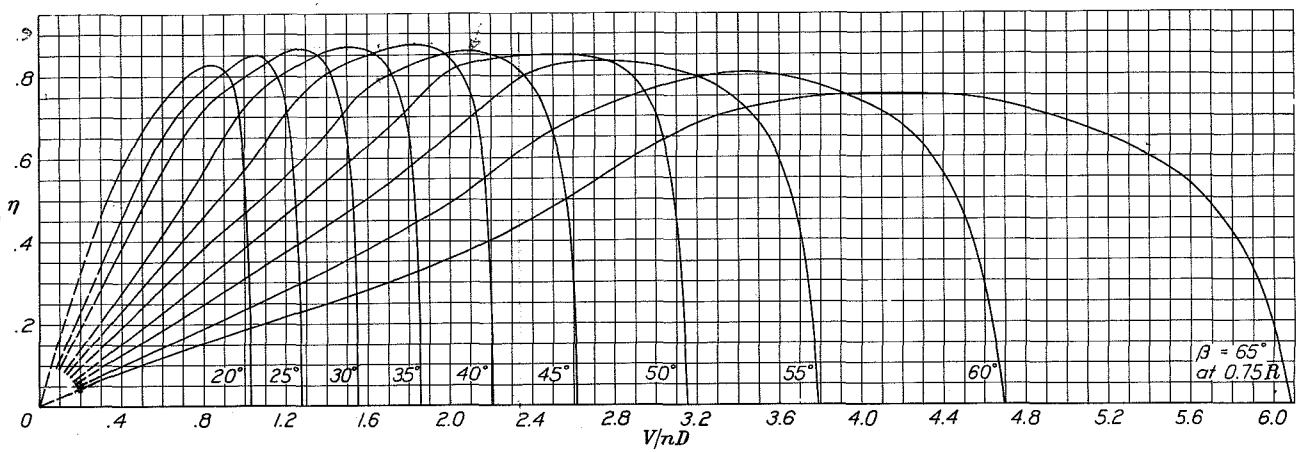

Figure 7.- Efficiency curves for four-blade single-rotation propeller without wing.

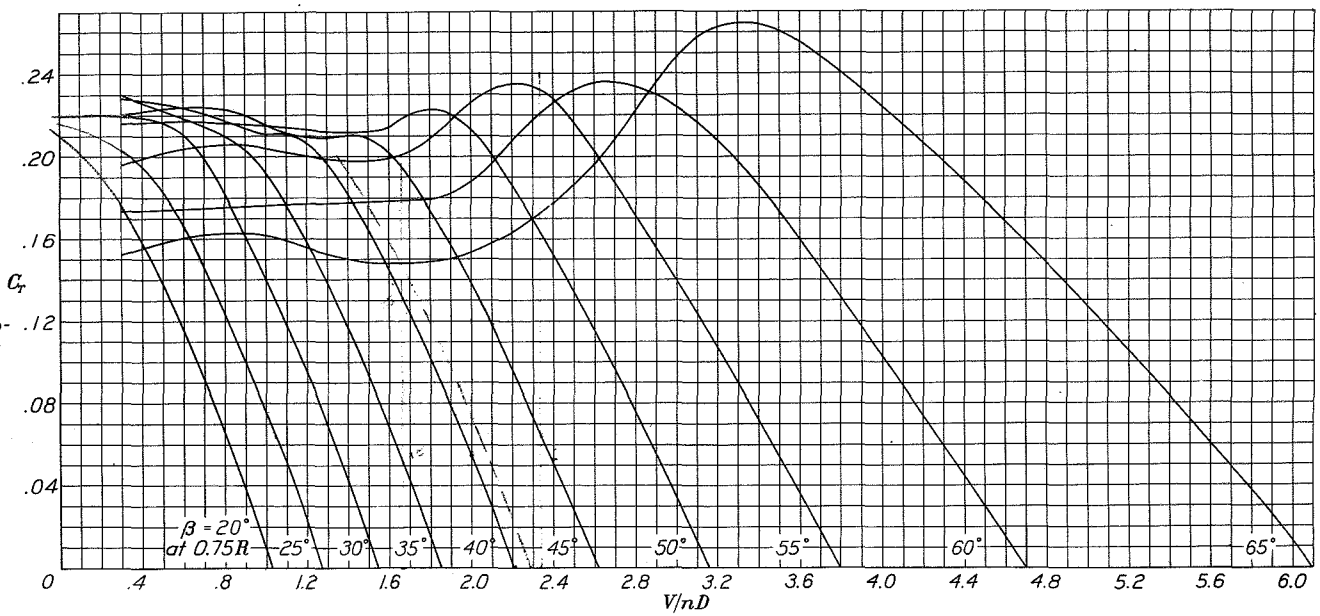

Figure 8.- Thrust-coefficient curves for four-blade single-rotation propeller without wing.

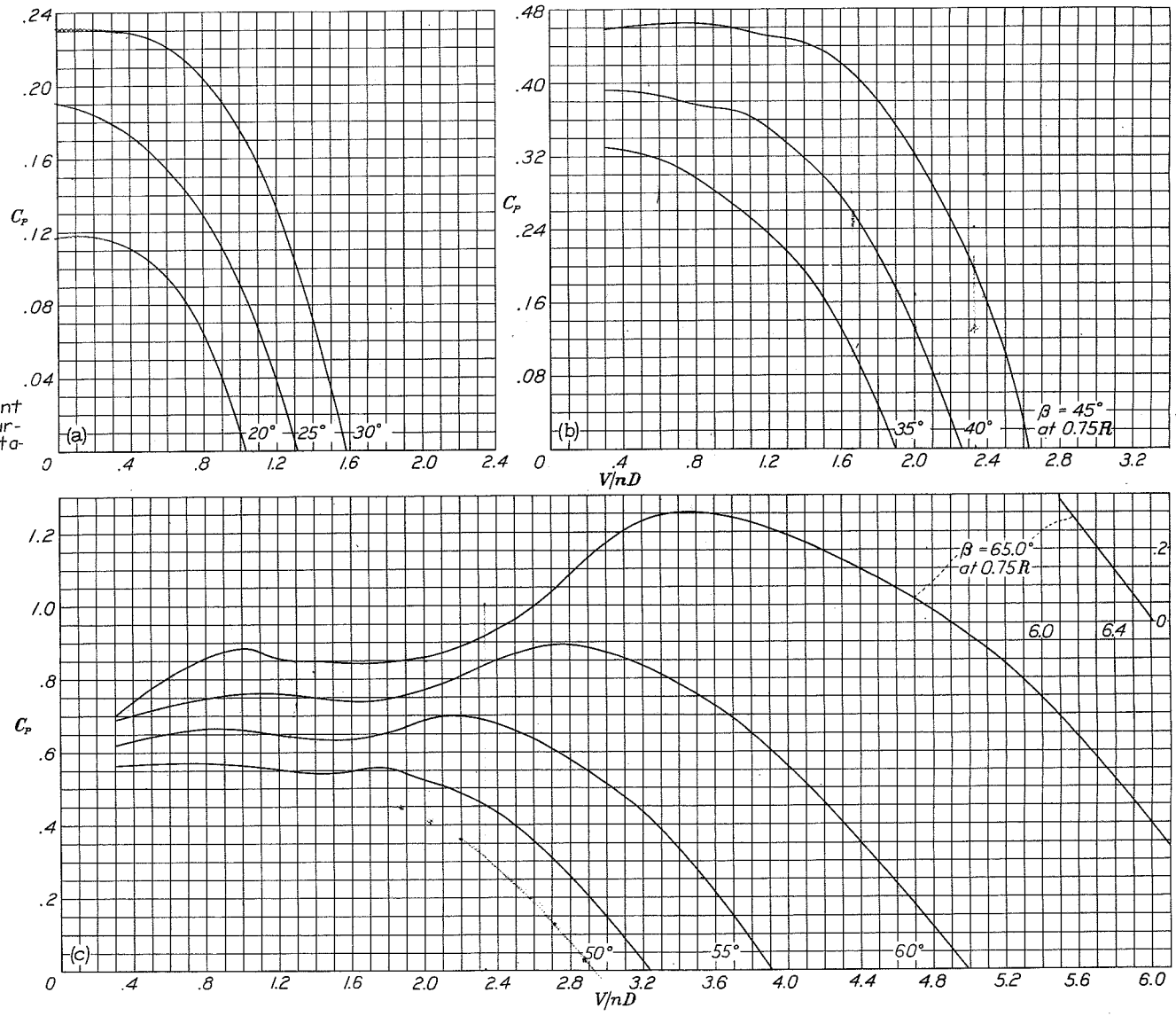

Figure 9a,b,c.- Power-coefficient curves for four-blade single-rotation propeller without wing.

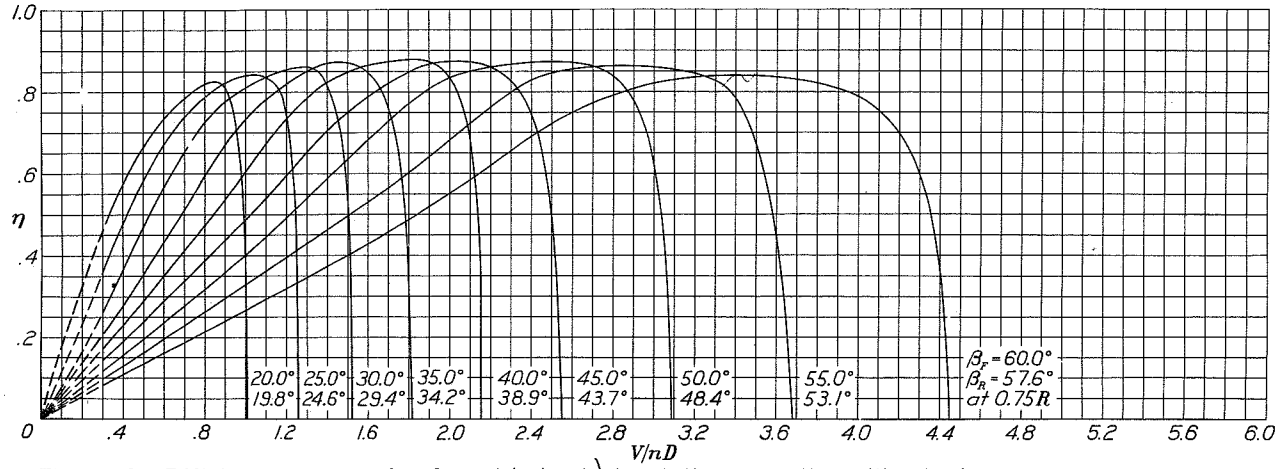

Figure 10.- Efficiency curves for four-blade dual-rotation propeller without wing.

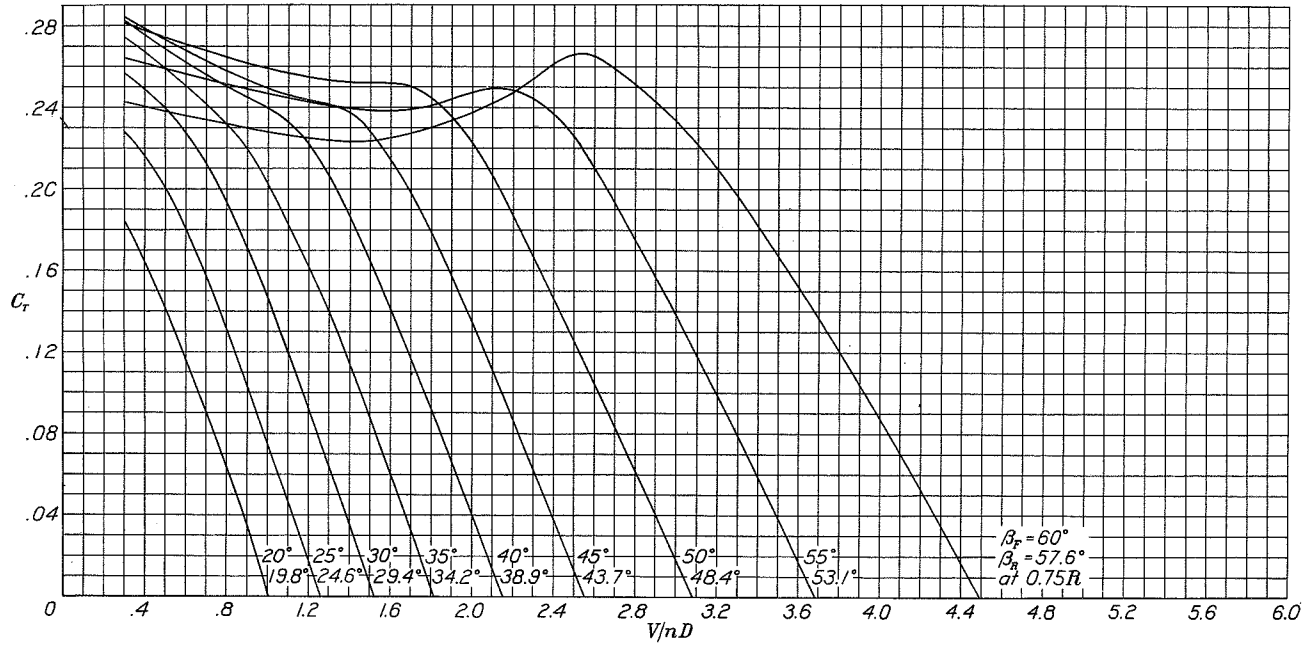

Figure 11.- Thrust-coefficient curves for four-blade dual-rotation propellers without wing.

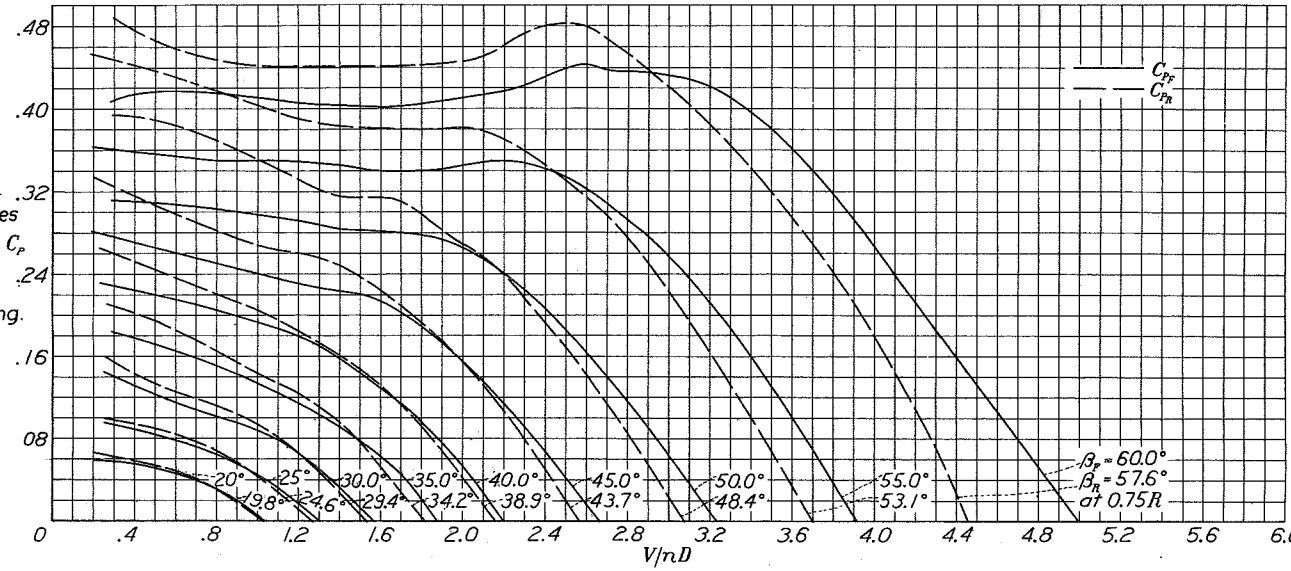

Figure 12.- Individual power-coefficient curves for four-blade dual-rotation propellers without wing.

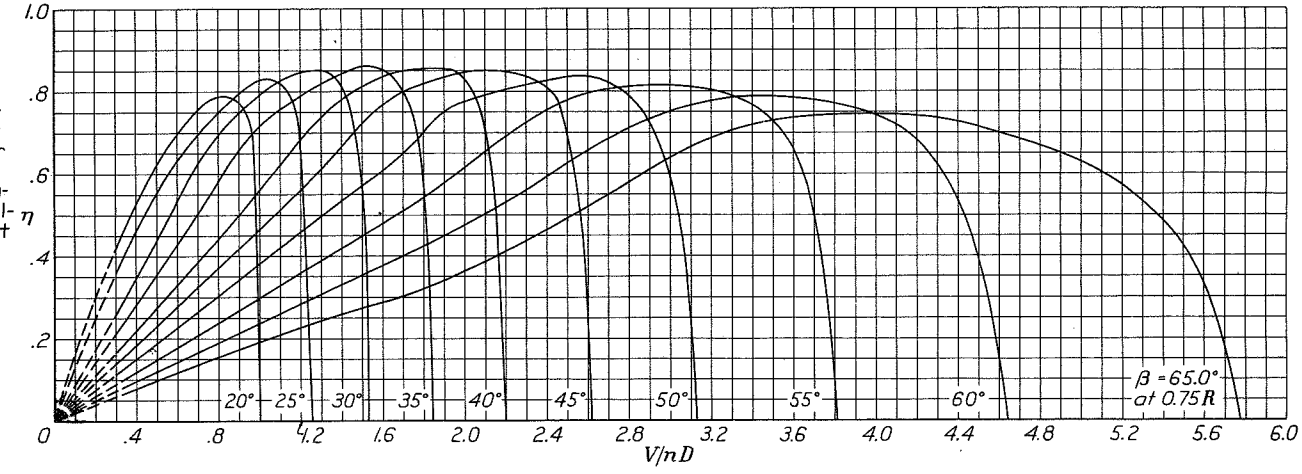

Figure 14.- Efficiency curves for six-blade single-rotation propellers without wing.

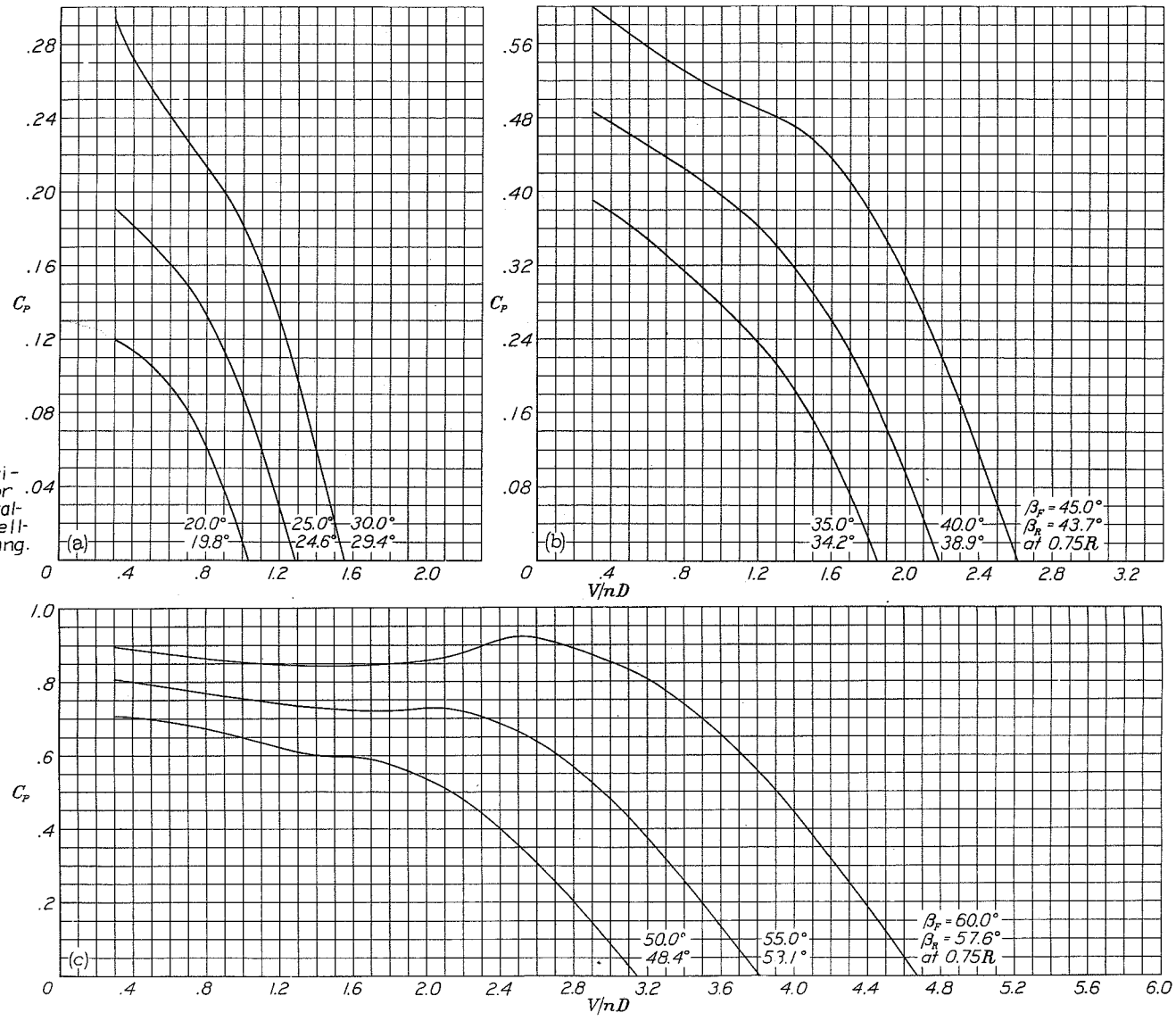

Figure 13 a,b,c.- Power-coefficient curves for four-blade dual-rotation propellers without wing.

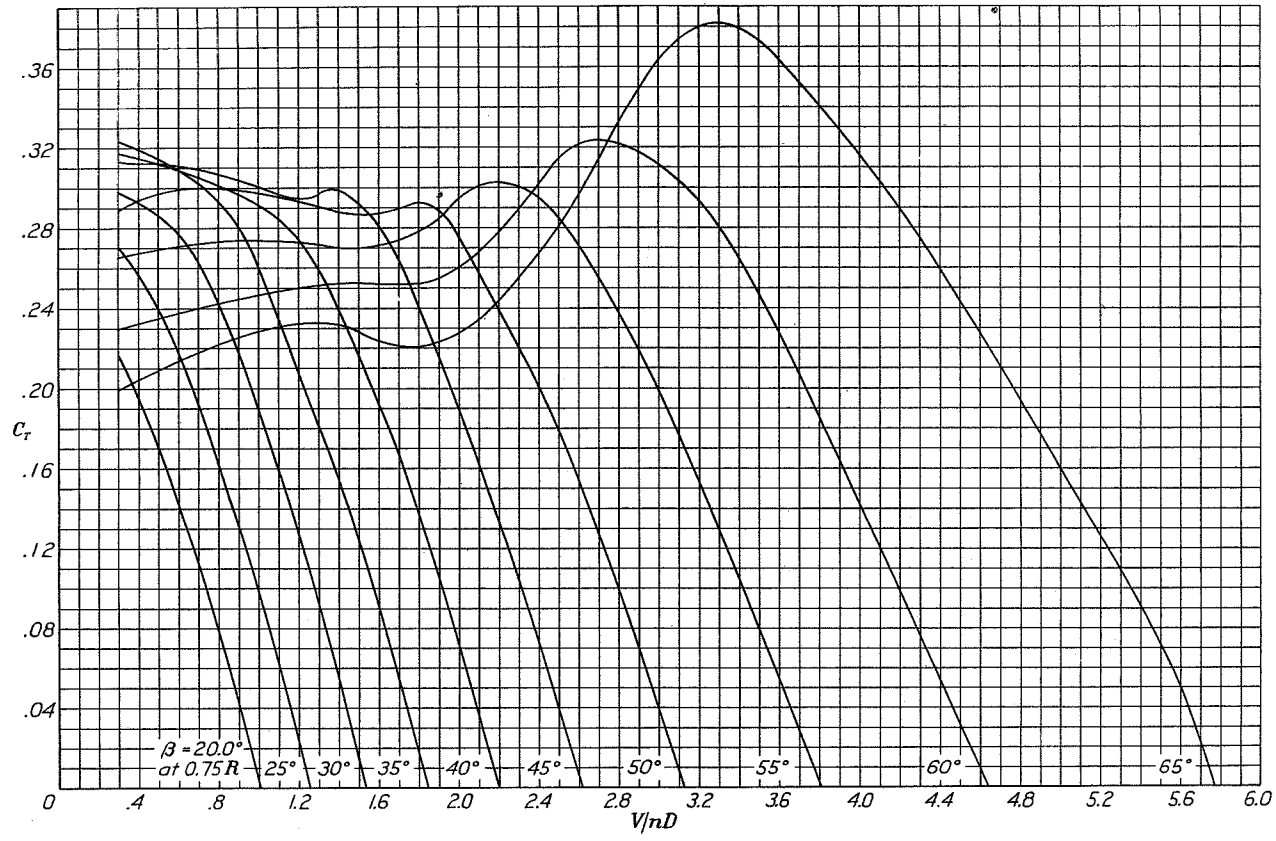

Figure 15.- Thrust-coefficient curves for six-blade single-rotation propeller without wing.

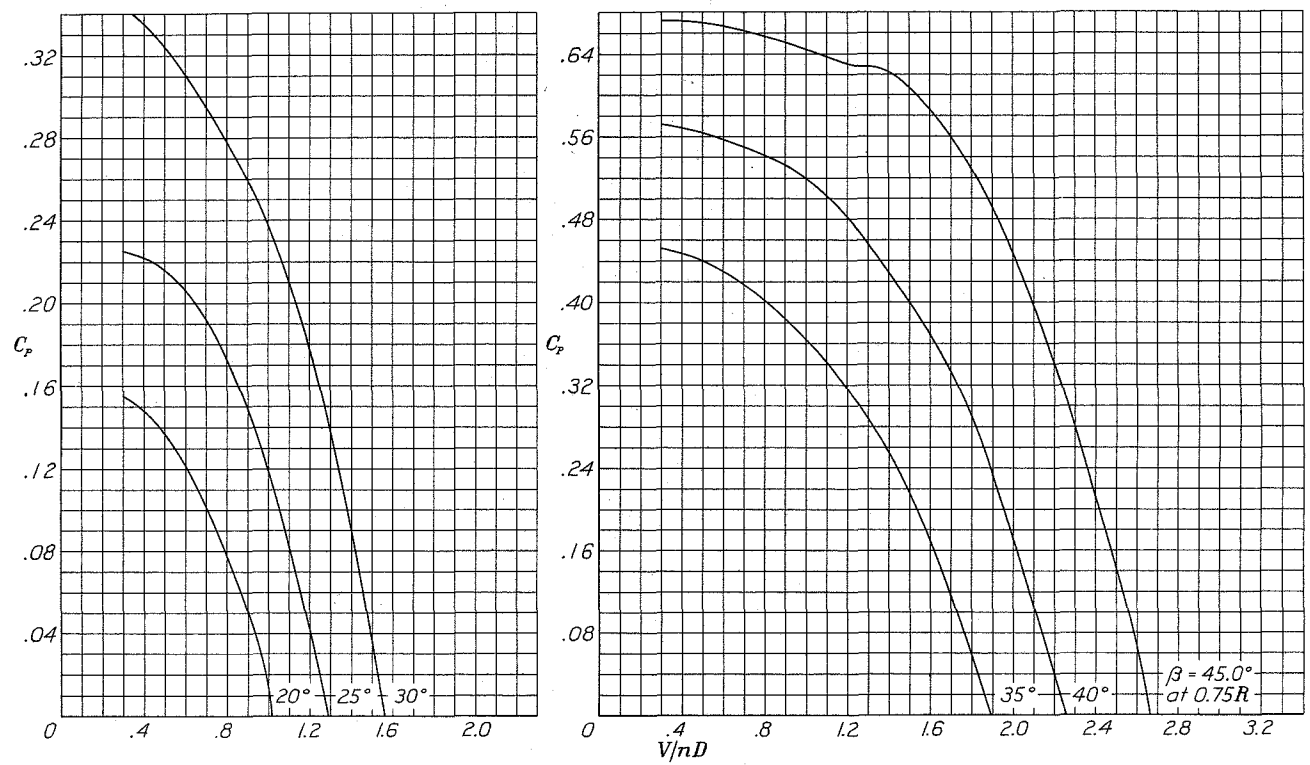

Figure 16a to c.- Power-coefficient curves for six-blade single-rotation propeller without wing.

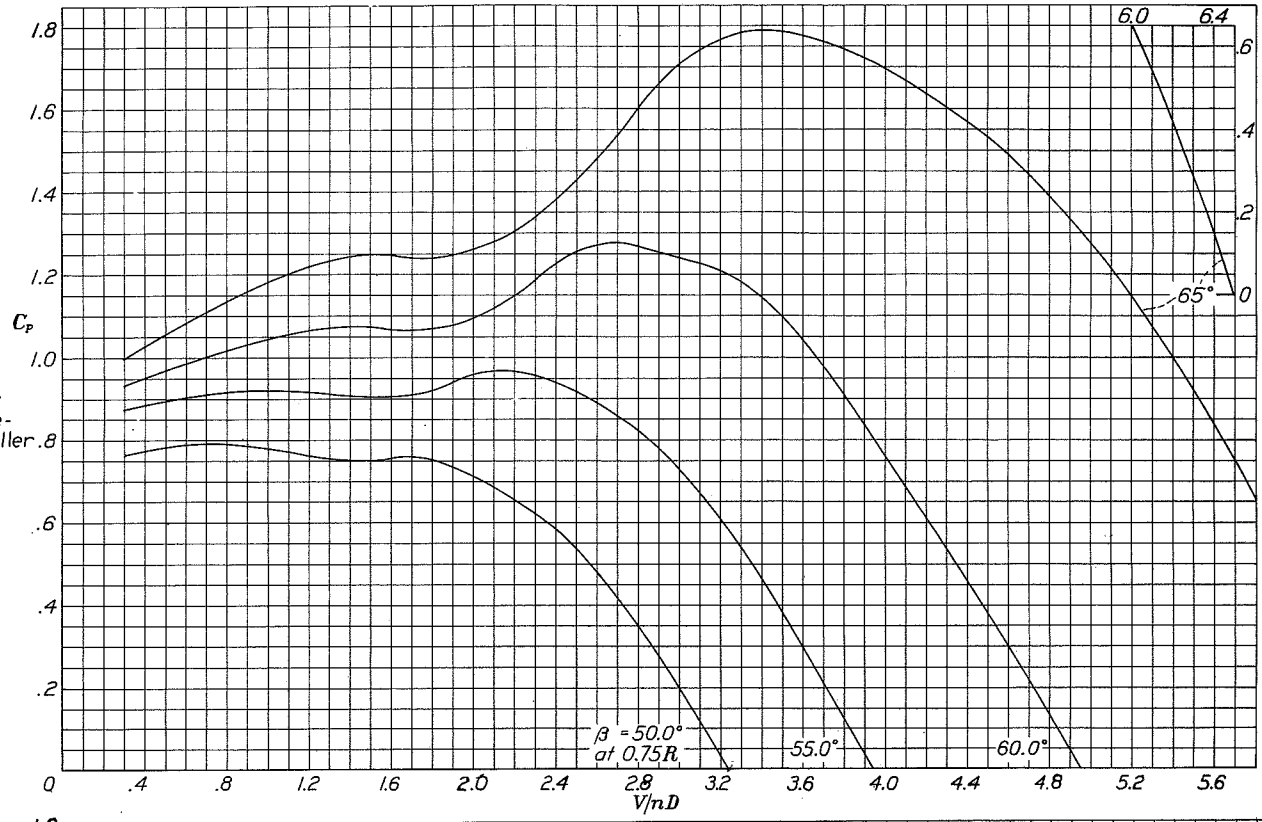

Figure 16c.- Power coefficient curves for six-blade single-rotation propeller without wing.

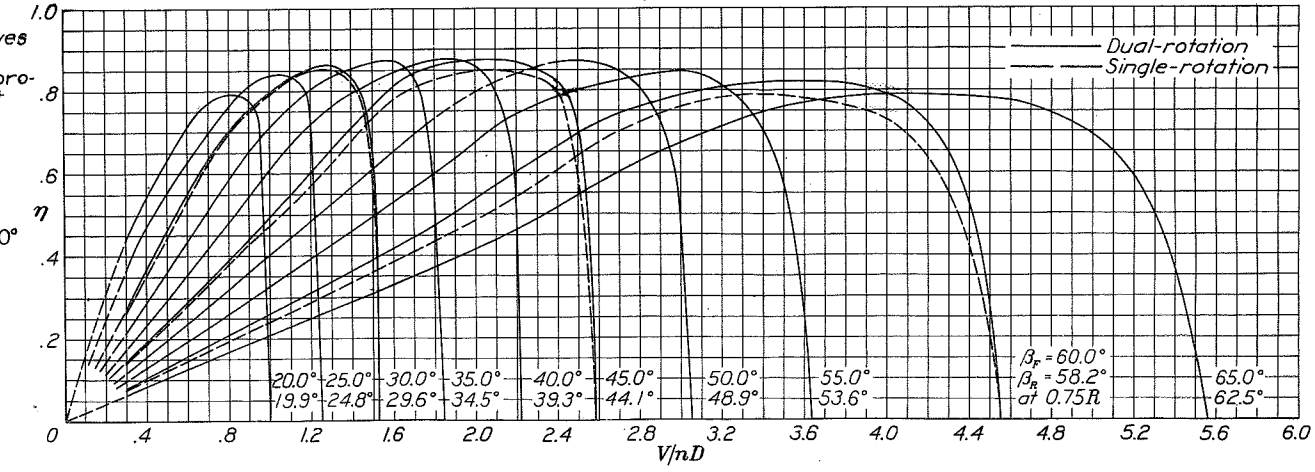

Figure 17.- Efficiency curves for six-blade dual-rotation propellers without wing, showing superimposed curves for the corresponding single-rotation condition at 30°, 45°, and 60° blade angles.

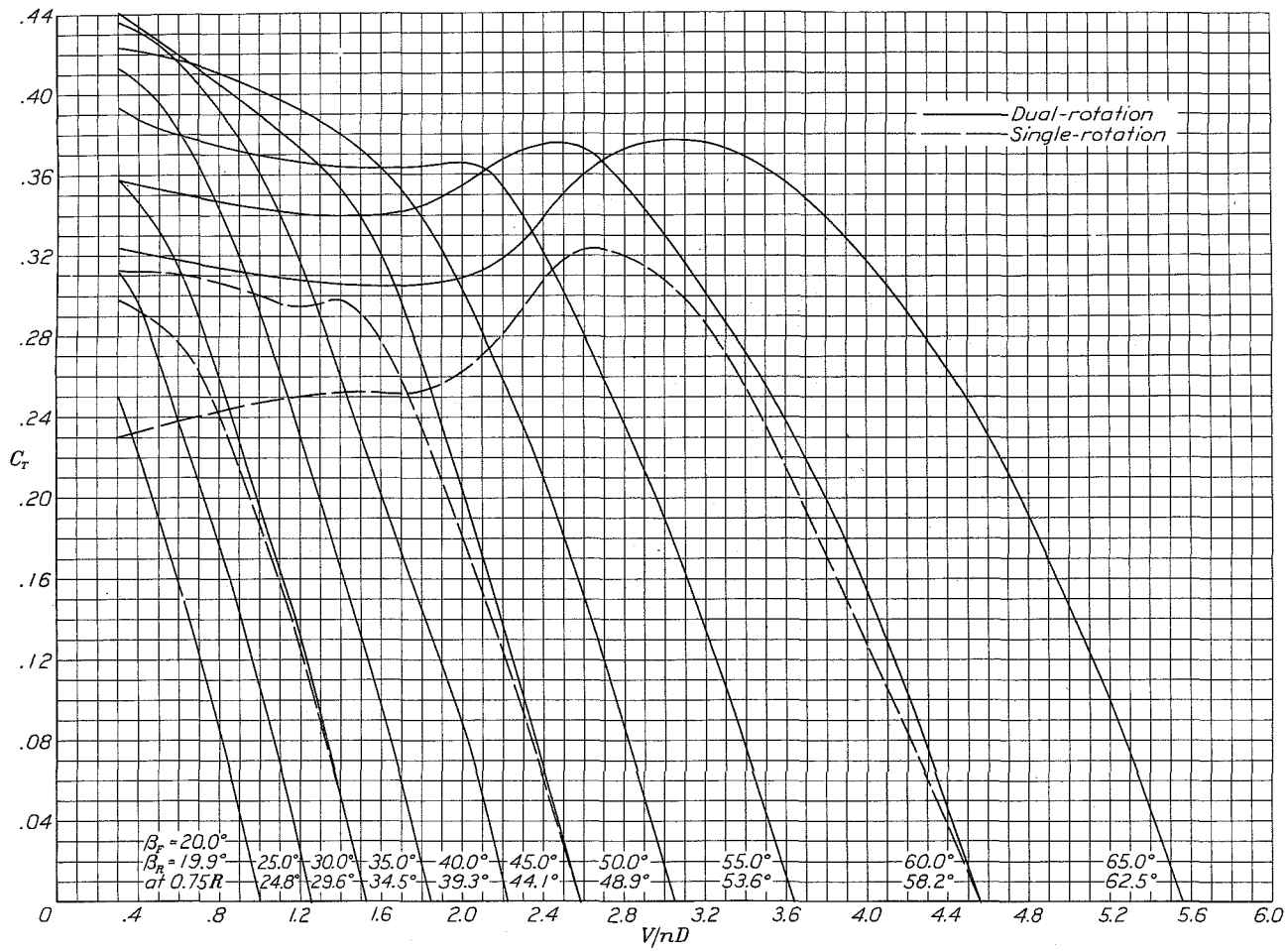

Figure 18.- Thrust-coefficient curves for six-blade dual-rotation propellers without wing, showing superimposed curves for the corresponding single-rotation condition at 30°, 45°, and 60° blade angles.

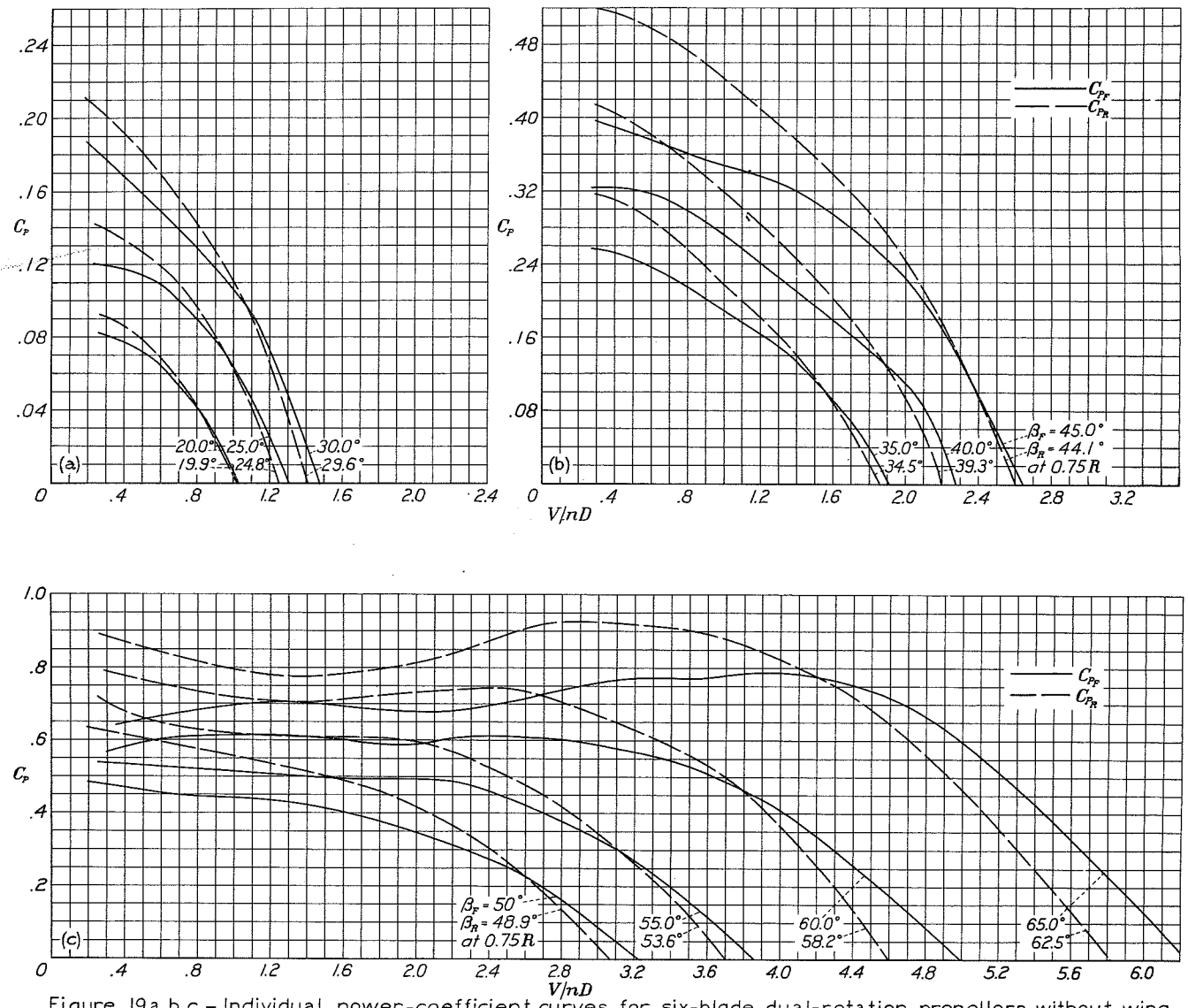

Figure 19a,b,c.- Individual power-coefficient curves for six-blade dual-rotation propellers without wing.

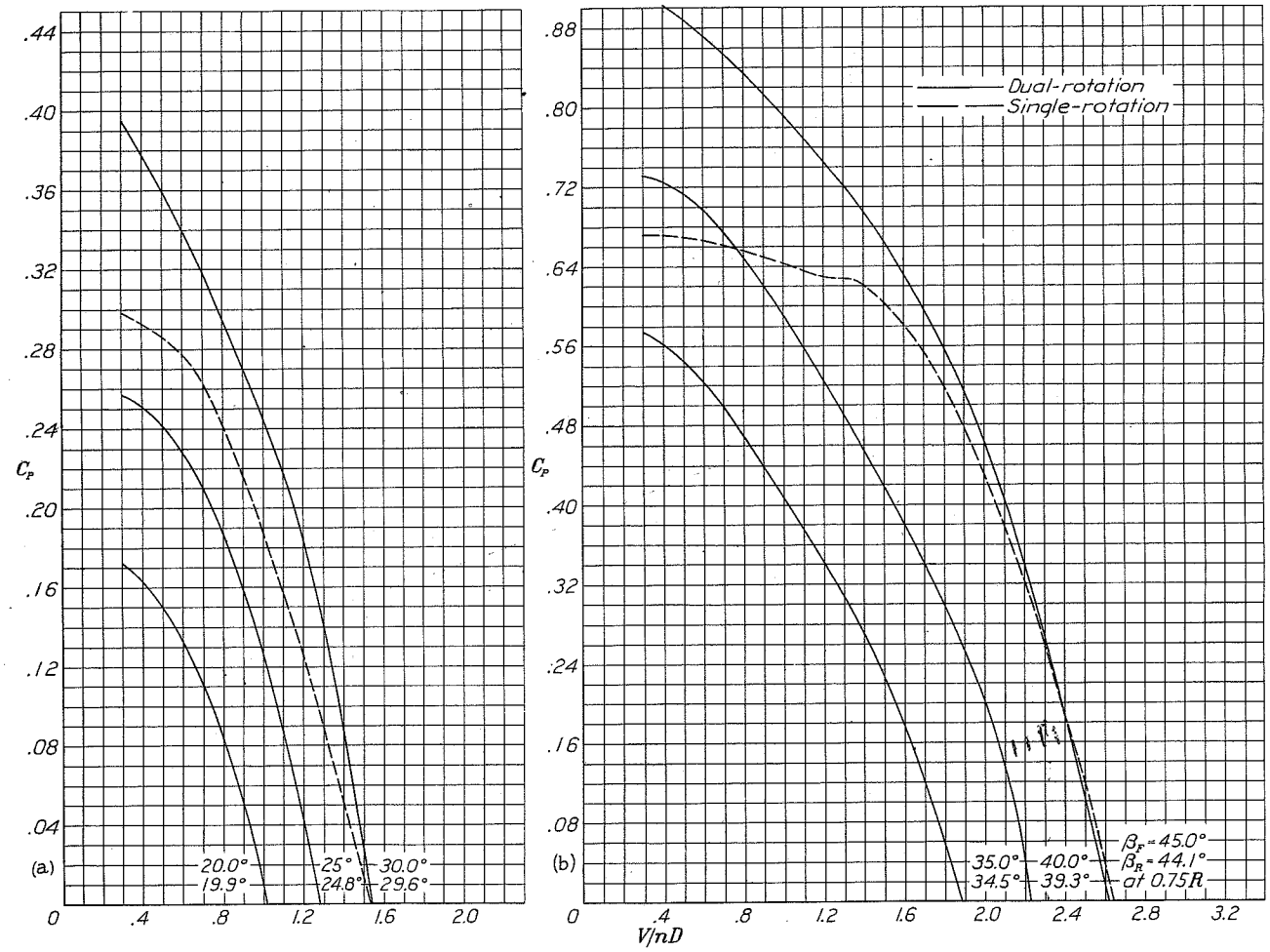

Figure 20 a,b. - Power-coefficient curves for six-blade dual-rotation propellers without wing, showing superimposed curve for the corresponding single-rotation condition. Fig. 20a at 30° blade angle, Fig. 20b at 45° blade angle.

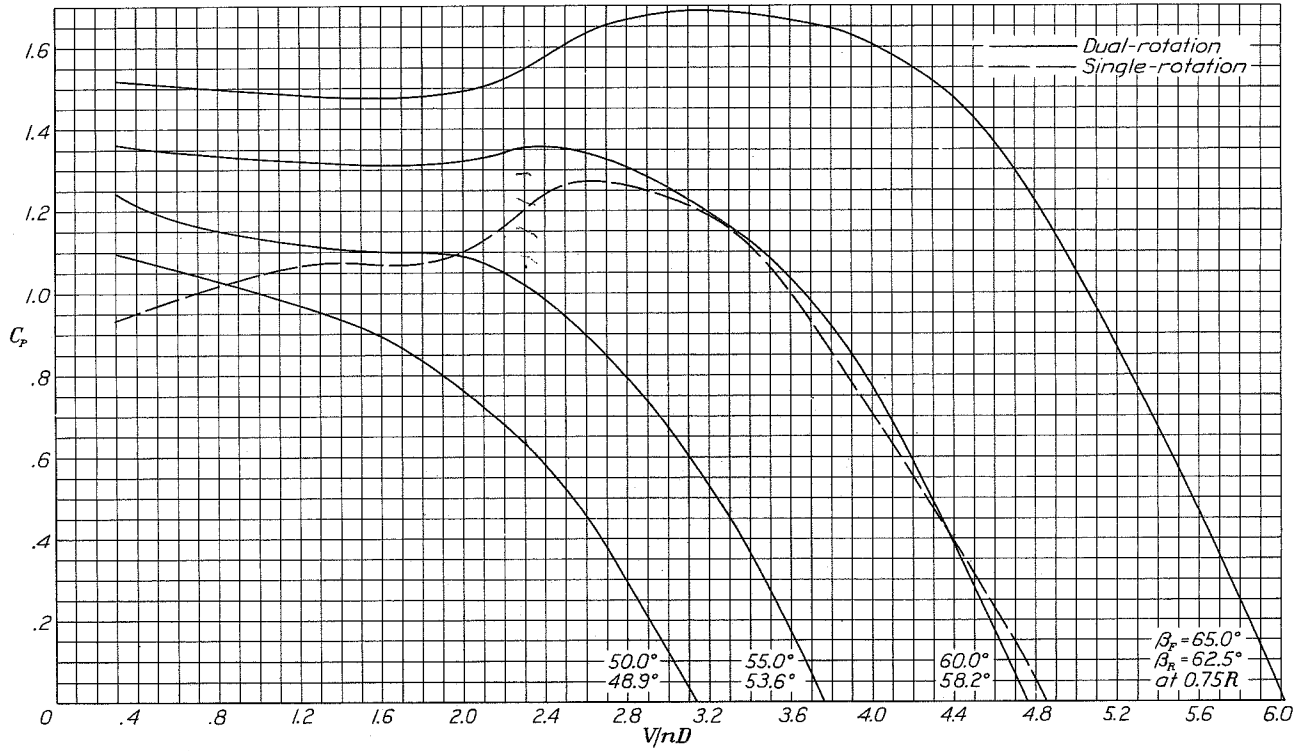

Figure 20c.- Power-coefficient curves for six-blade dual-rotation propellers without wing, showing superimposed curve for the corresponding single-rotation condition at 60° blade angle.

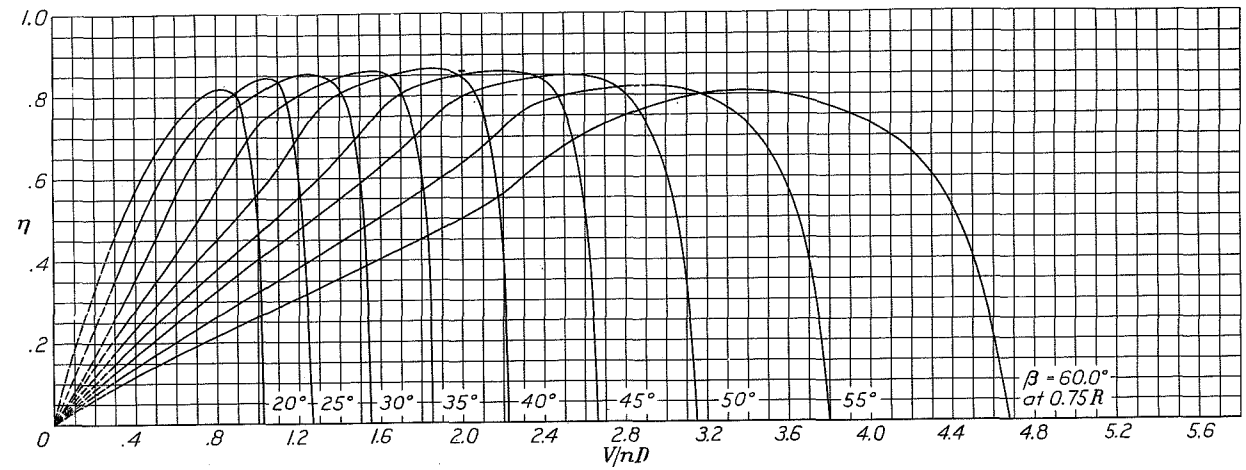

Figure 21.- Efficiency curves for four-blade single-rotation propeller with wing.

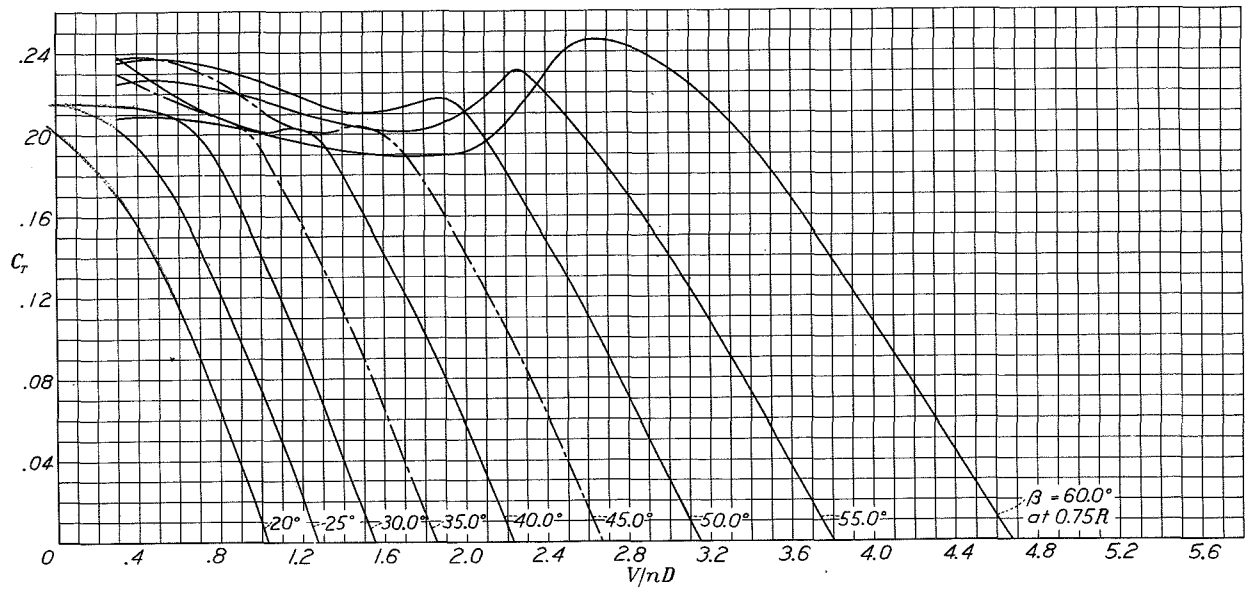

Figure 22.- Thrust-coefficient curves for four-blade single-rotation propeller with wing.

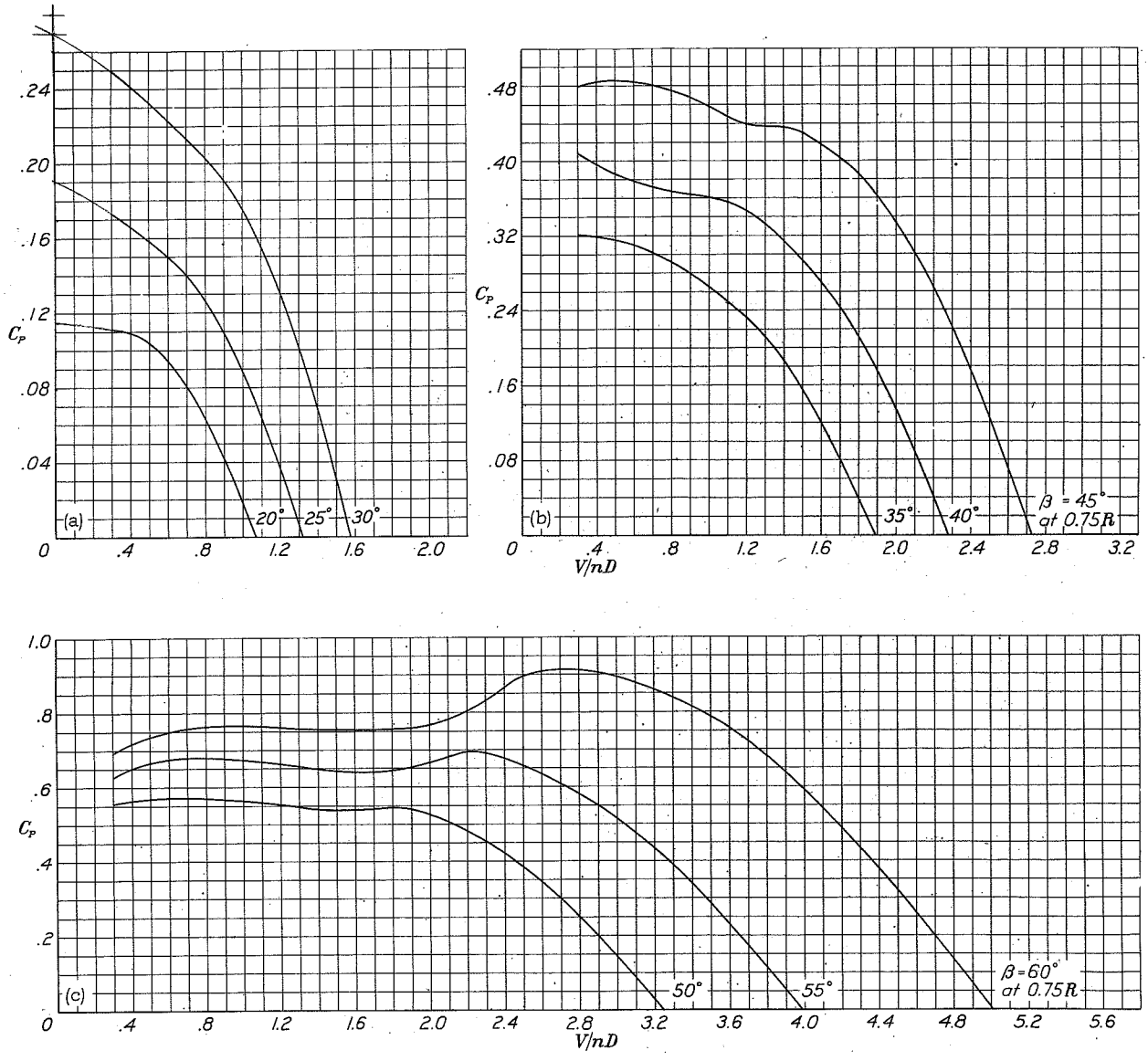

Figure 23.- Power-coefficient curves for four-blade single-rotation propeller with wing.

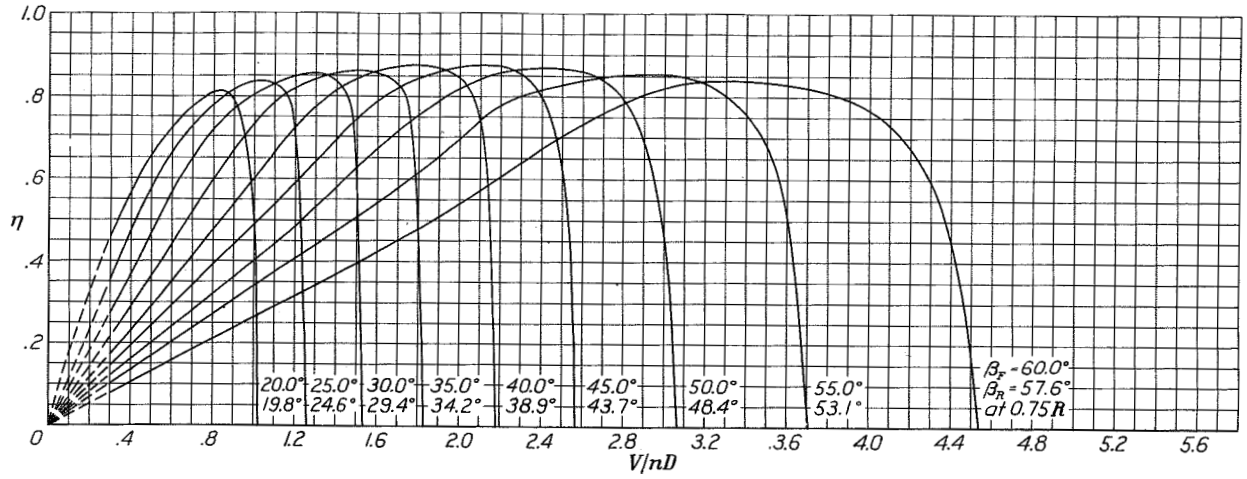

Figure 24.- Efficiency curves for four-blade dual-rotation propellers with wing.

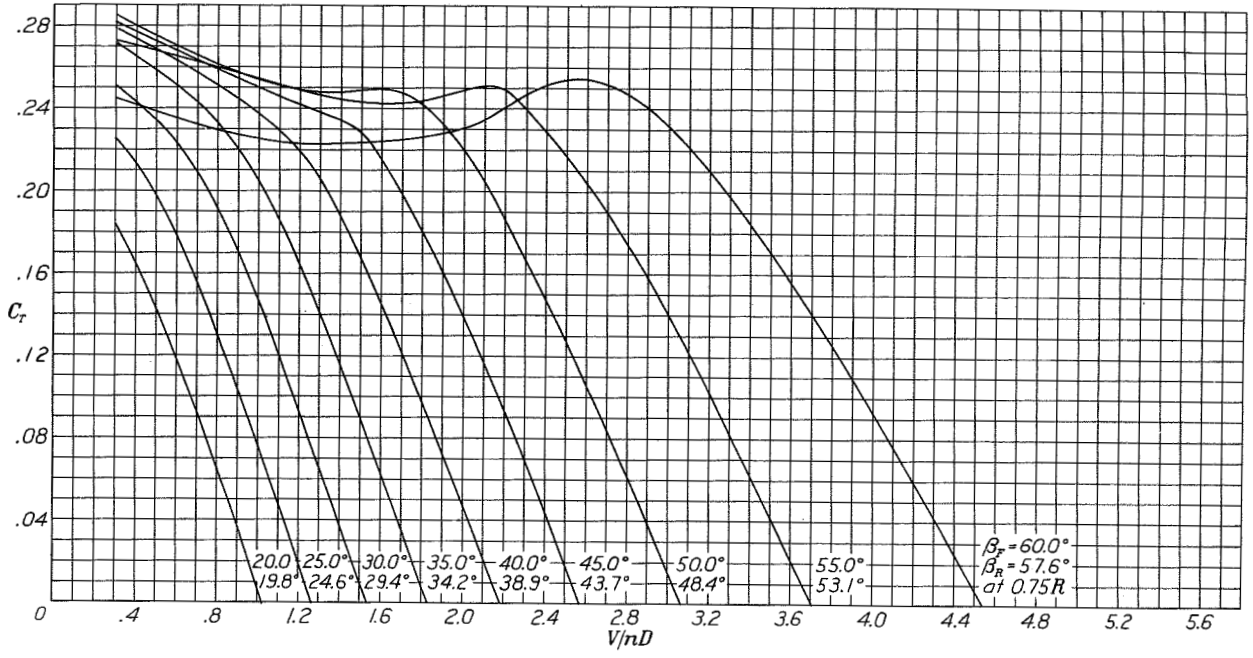

Figure 25.- Thrust-coefficient curves for four-blade dual-rotation propellers with wing.

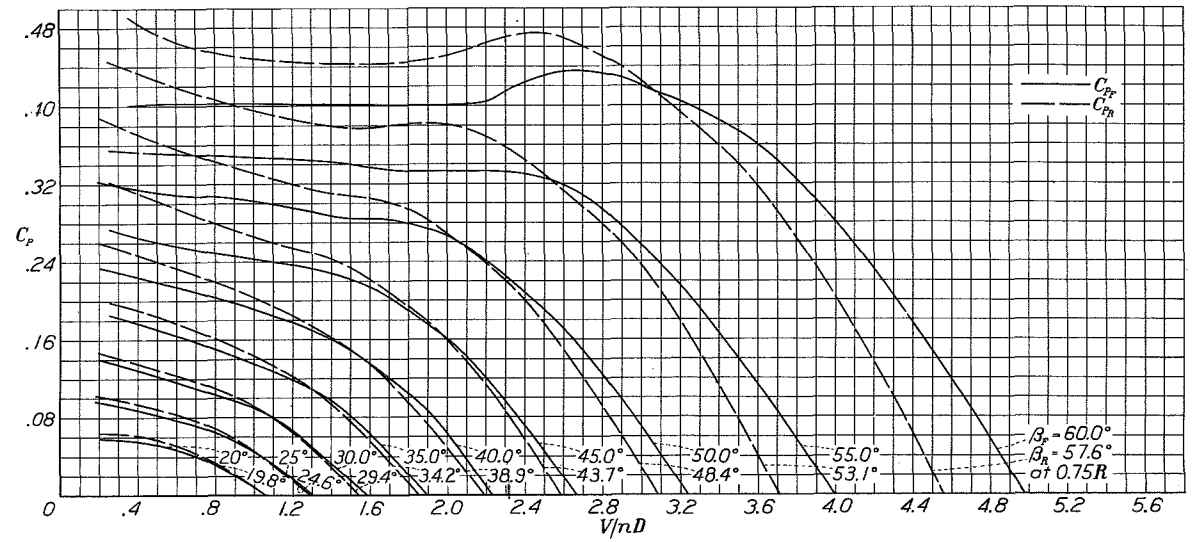

Figure 26.- Individual power-coefficient curves for four-blade dual-rotation propellers with wing.

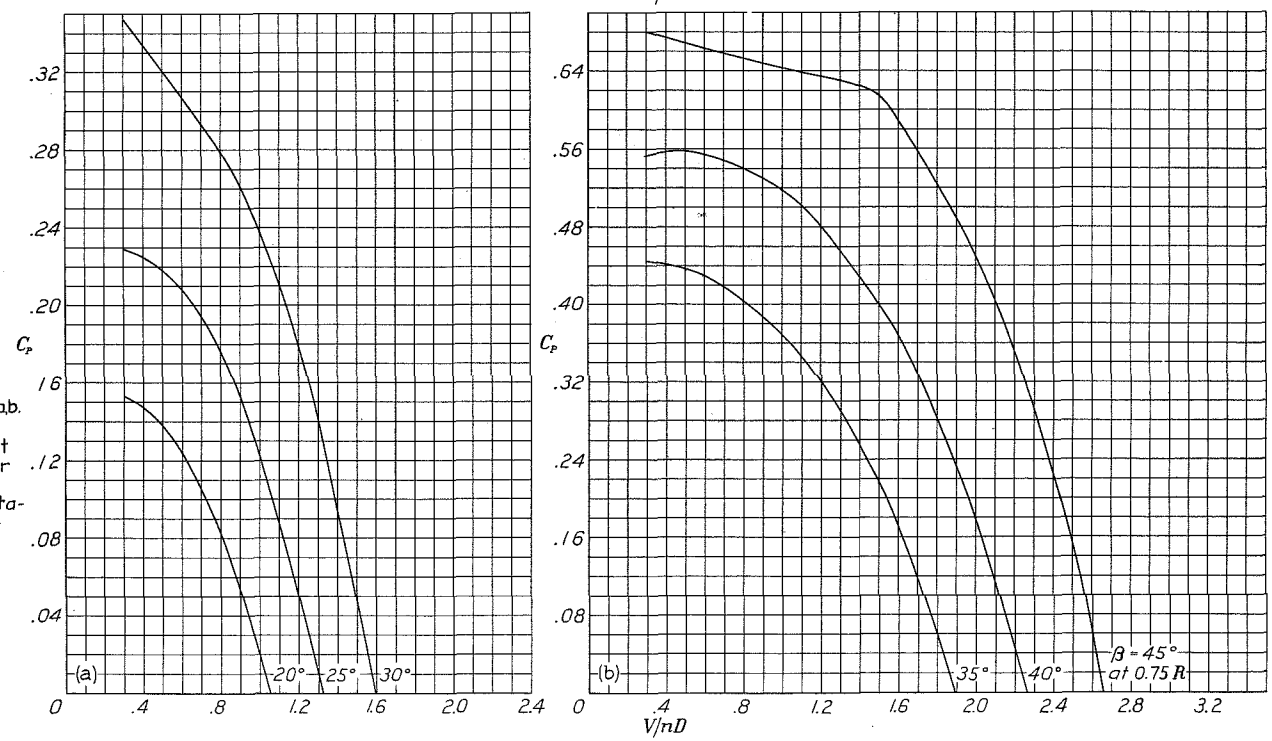

Figure 30a,b. Power-coefficient curves for six-blade single-rotation propeller with wing.

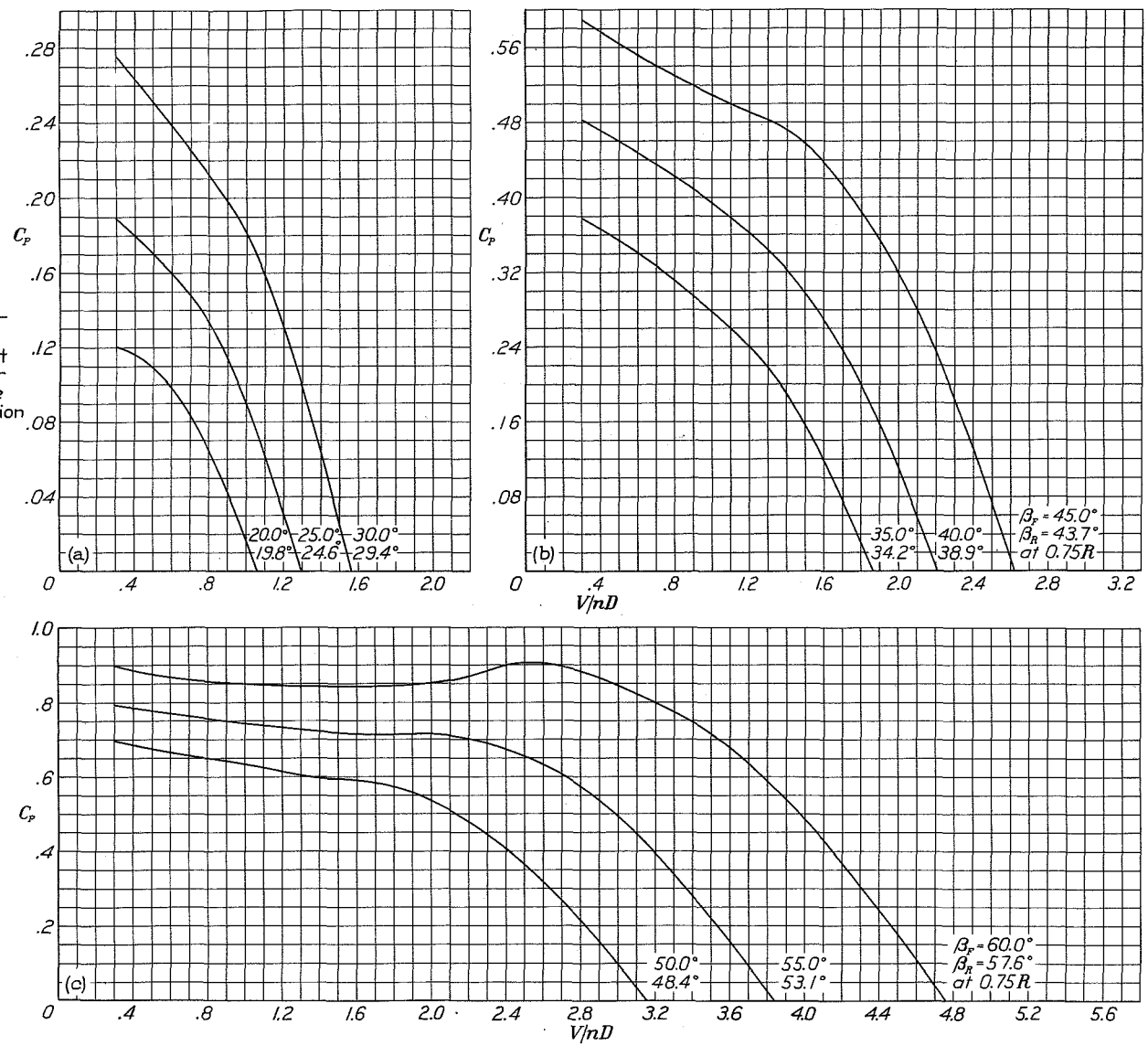

Figure 27. - Power-coefficient curves for four-blade dual-rotation propellers with wing.

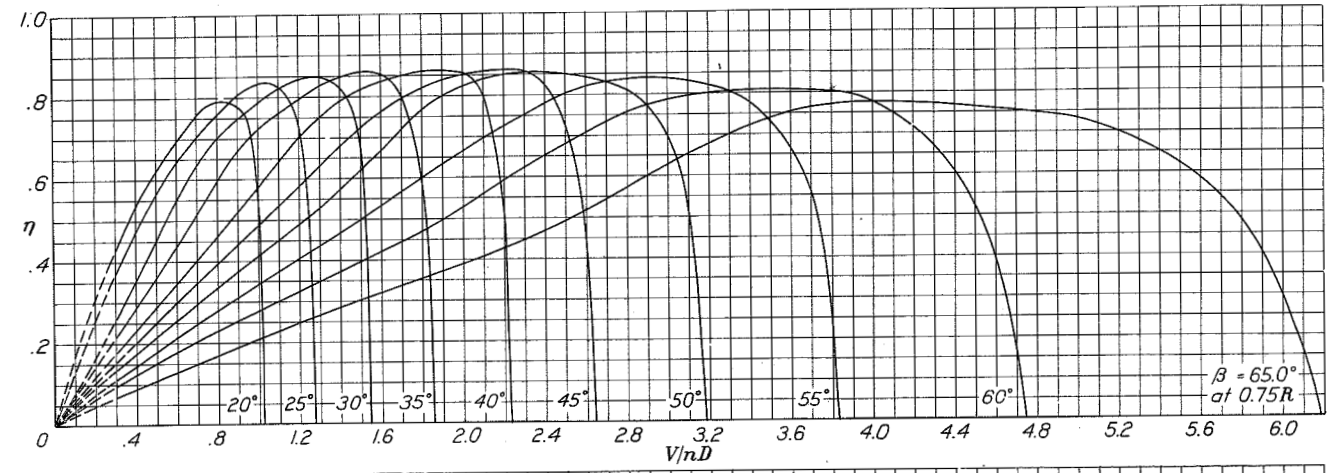

Figure 28.- Efficiency curves for six-blade single-rotation propeller with wing.

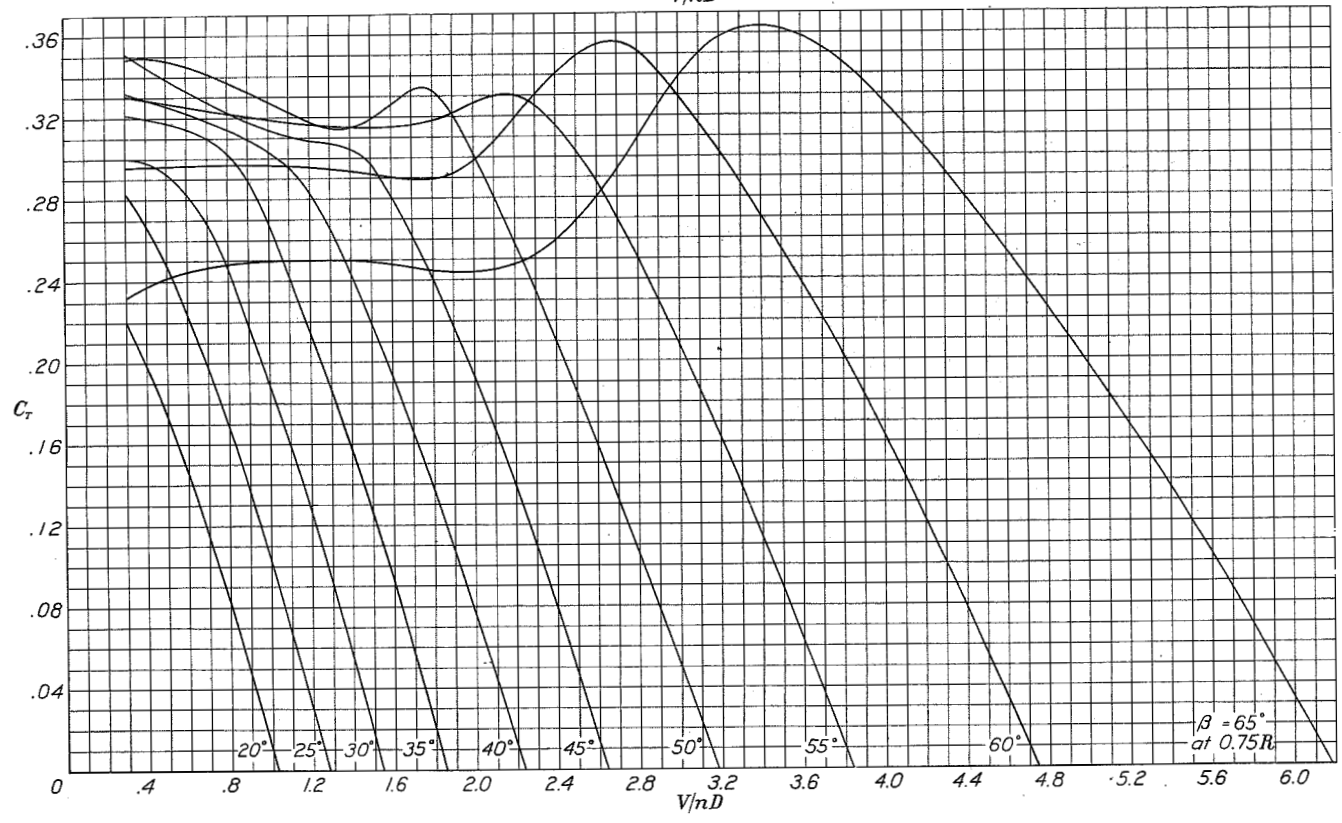

Figure 29.- Thrust-coefficient curves for six-blade single-rotation propeller with wing.

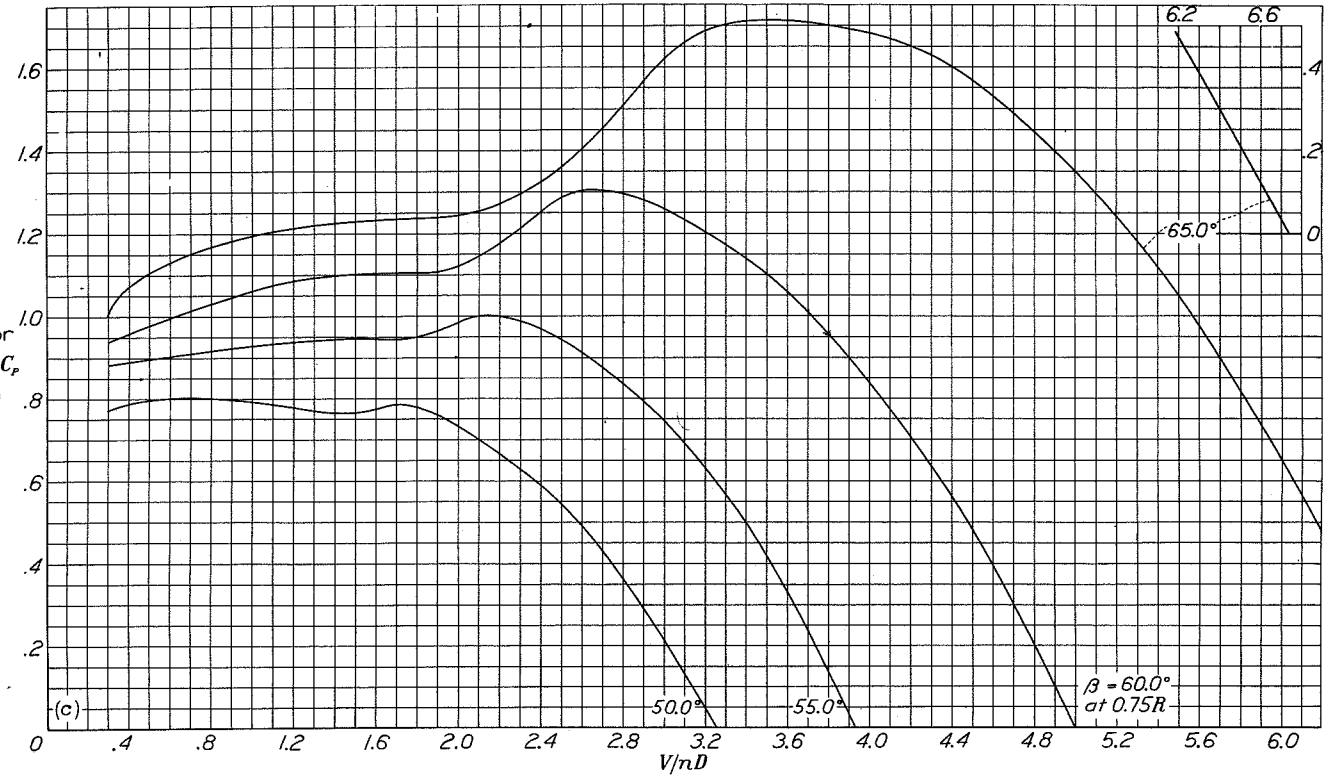

Figure 30 c.- Power-coefficient curves for six-blade single-rotation propeller with wing.

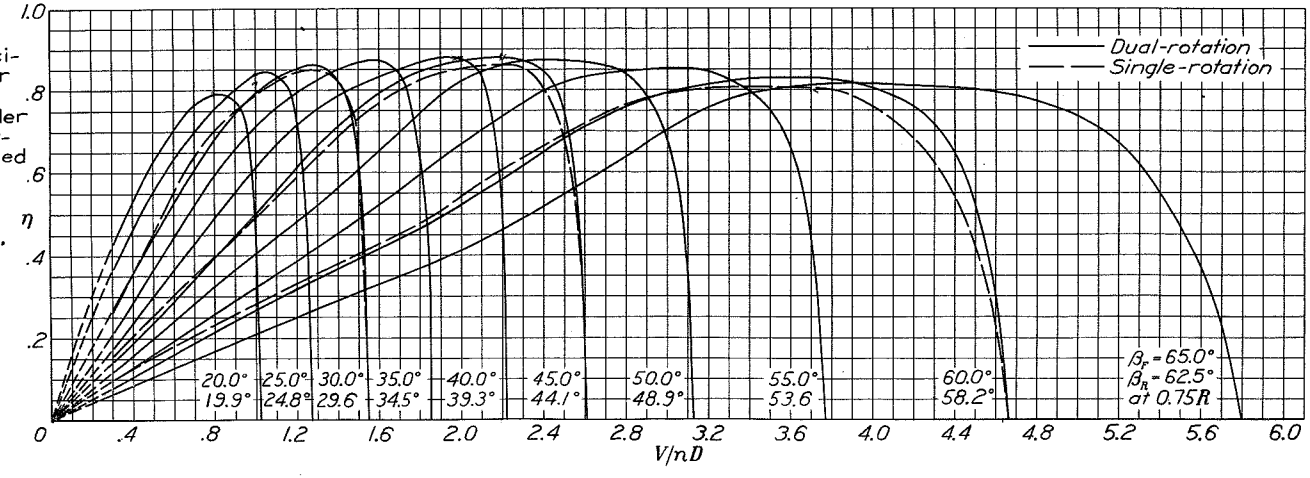

Figure 31.- Efficiency curves for six-blade dual-rotation propeller with wing, showing superimposed curves for the corresponding single-rotation condition at 30°, 45°, and 60° blade angles.

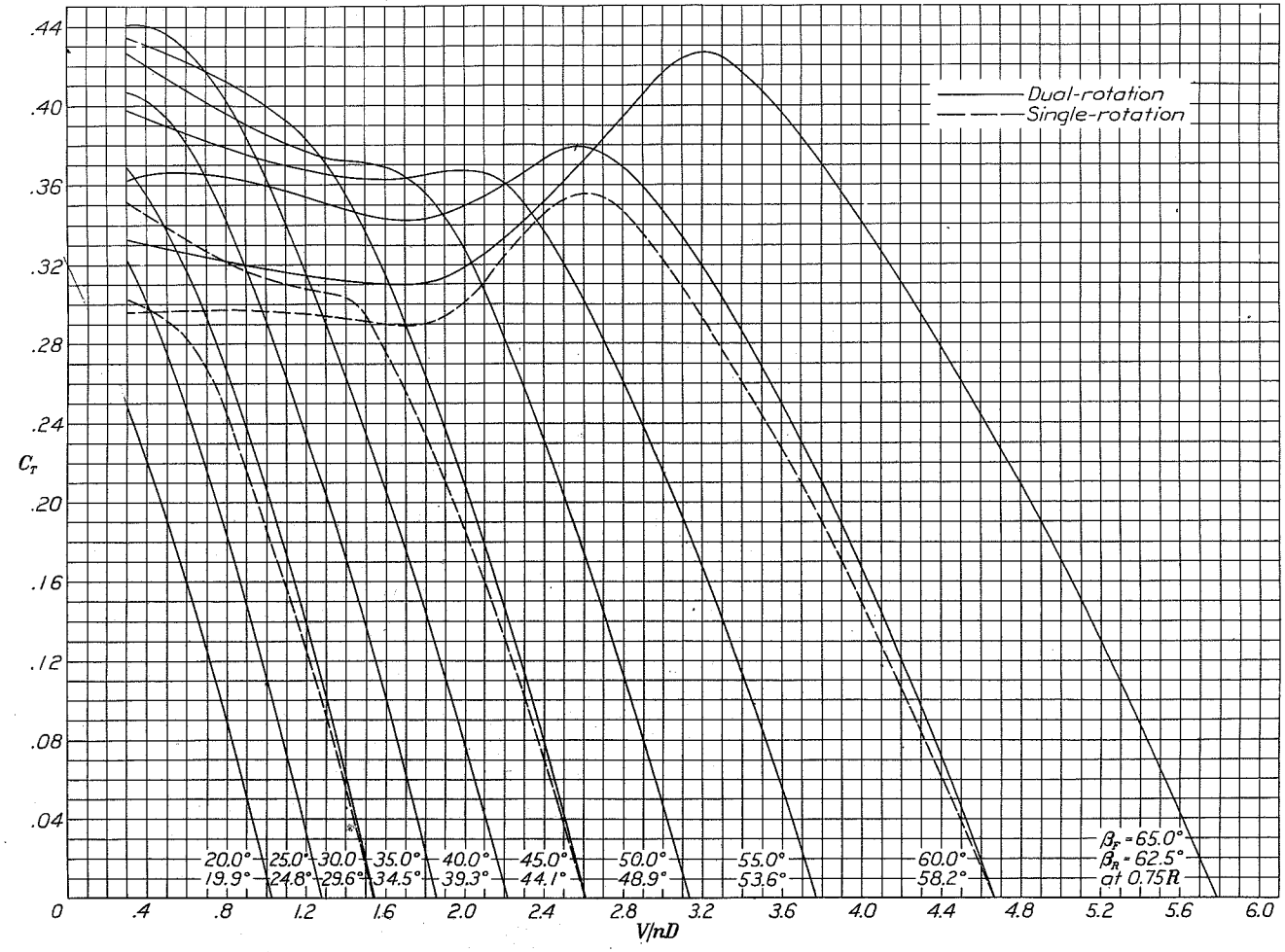

Figure 32.- Thrust-coefficient curves for six-blade dual-rotation propeller with wing, showing superimposed curves for the corresponding single-rotation condition at 30°, 45°, and 60° blade angles.

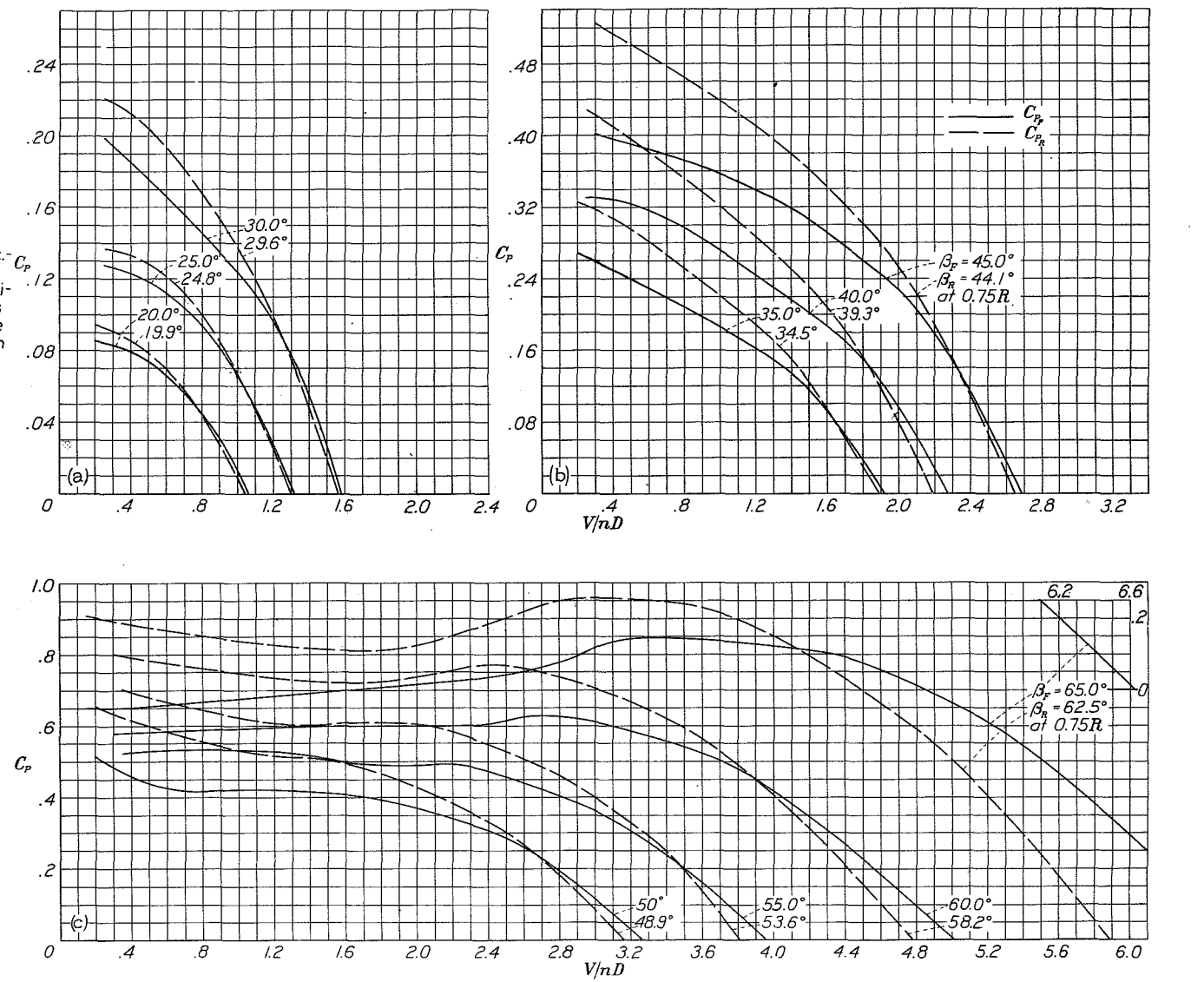

Figure 33a,b,c.- Individual power-coefficient curves for six-blade dual-rotation propellers with wing.

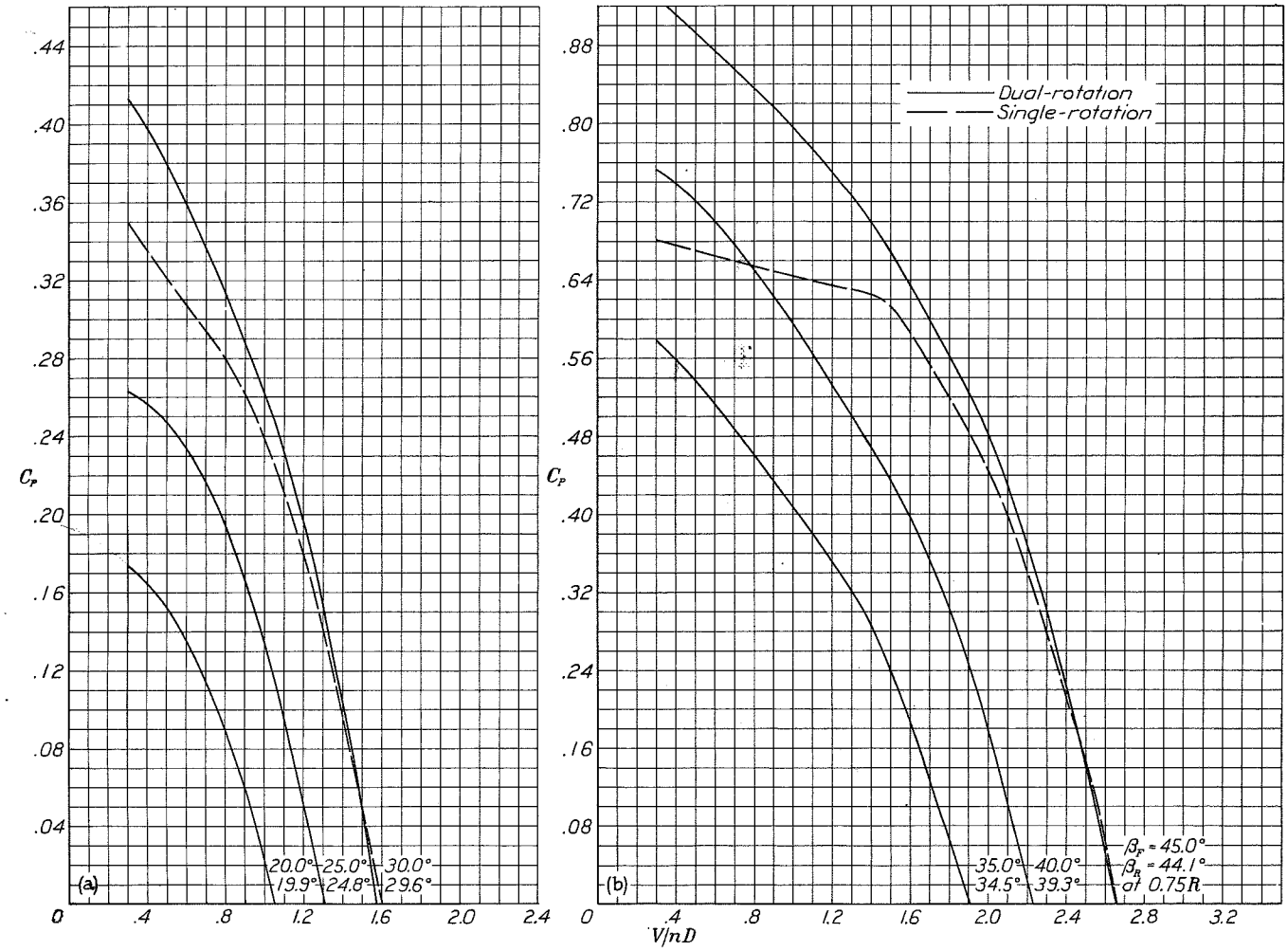

Figure 34 a,b.– Power-coefficient curves for six-blade dual-rotation propellers with wing, showing superimposed curve for the corresponding single-rotation condition, (a) at 30° blade angle, (b) at 45° blade angle.

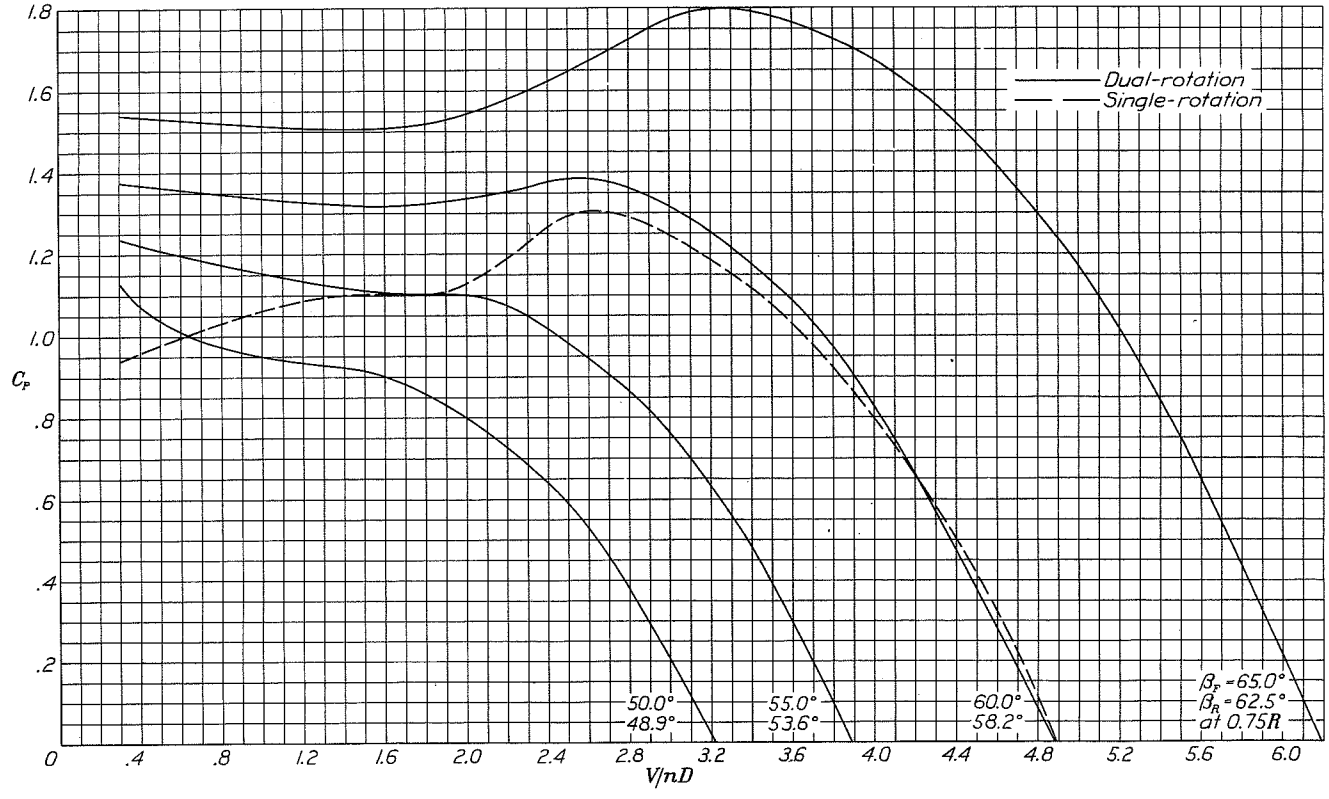

Figure 34c.- Power-coefficient curves for six-blade dual-rotation propellers with wing, showing superimposed curve for the corresponding single-rotation condition at 60° blade angle.

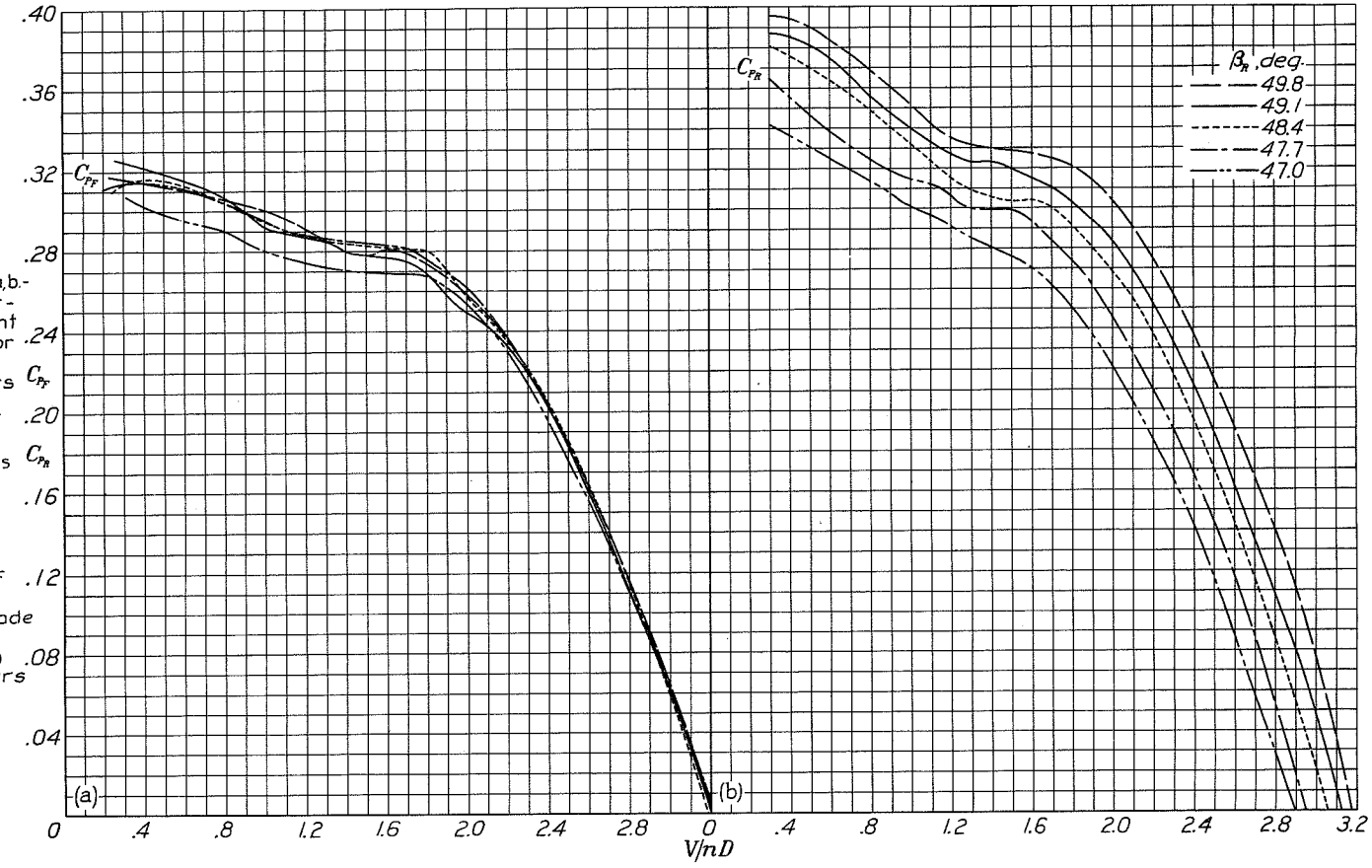

(a) For front propeller

(b) For rear propeller

Figure 35a,b.- Power-coefficient curves for the propellers showing effect of small variations in rear blade angle at a front blade angle of 50° (Four-blade dual-rotation propellers without wing).

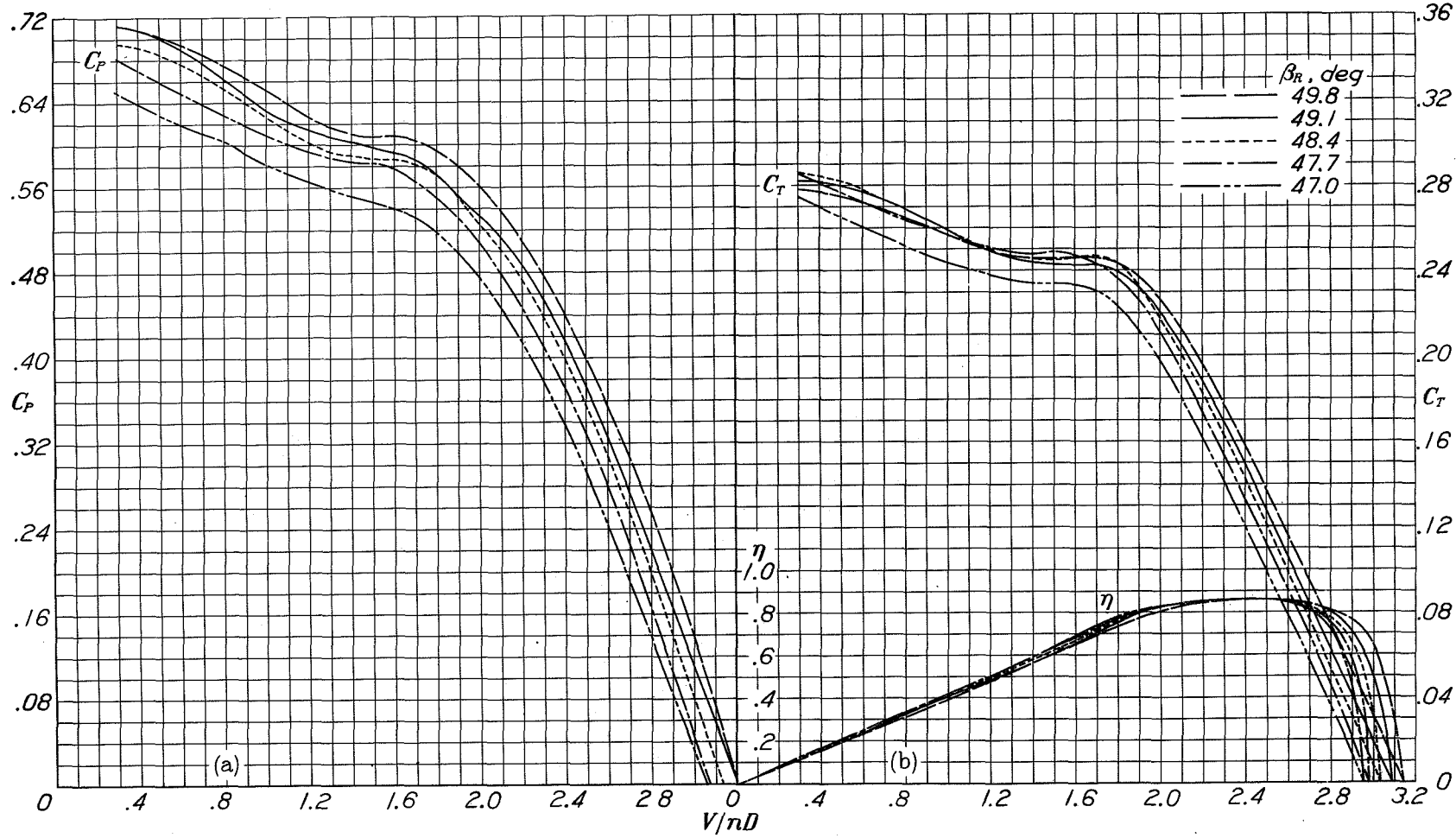

Figure 36.- Propeller curves showing the effect of small variations in rear blade angle at a front blade angle of 50°. (Four-blade dual-rotation propellers without wing.)

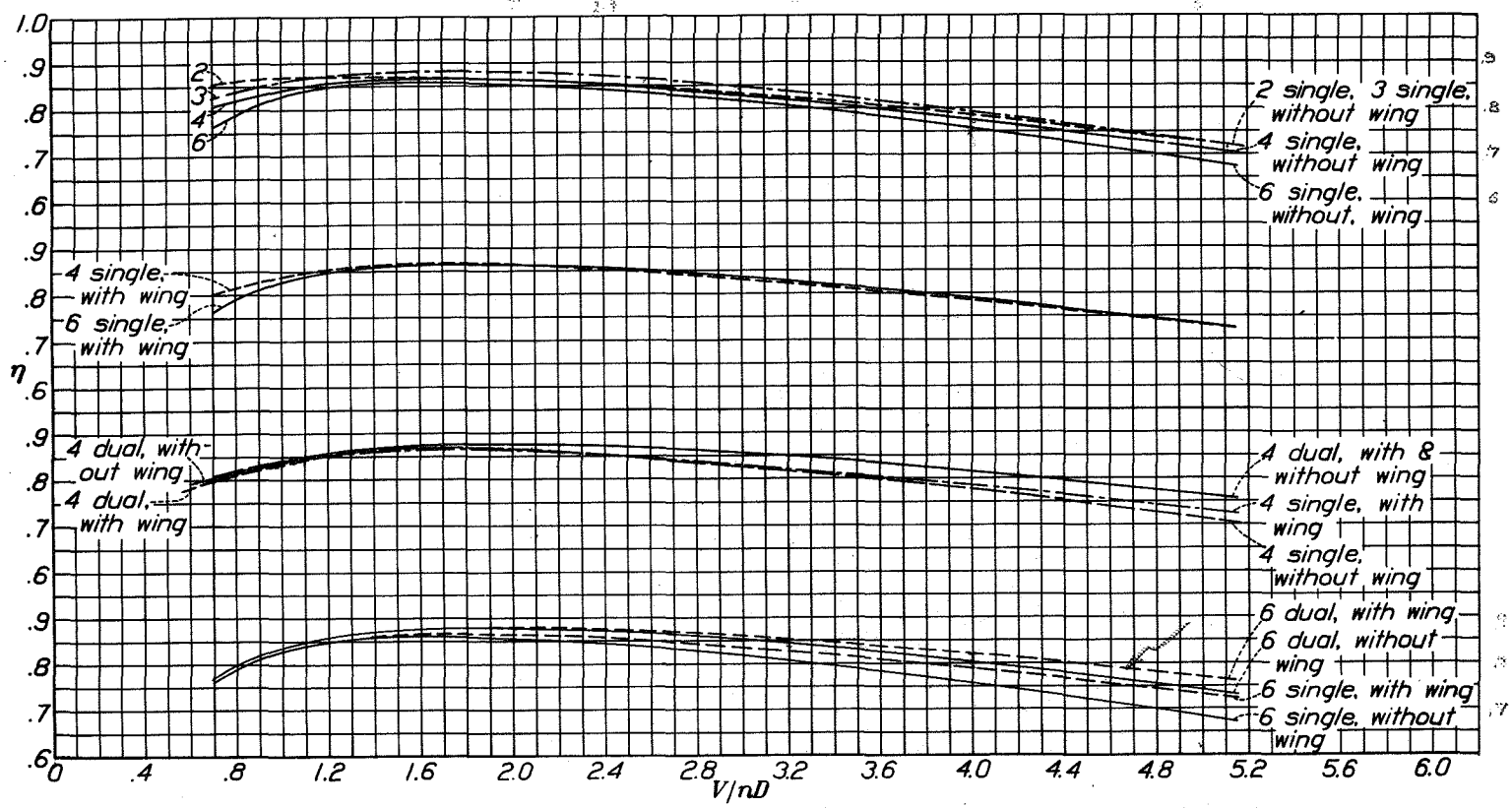

Figure 37.- Comparison of efficiency envelope curves for the propellers tested.

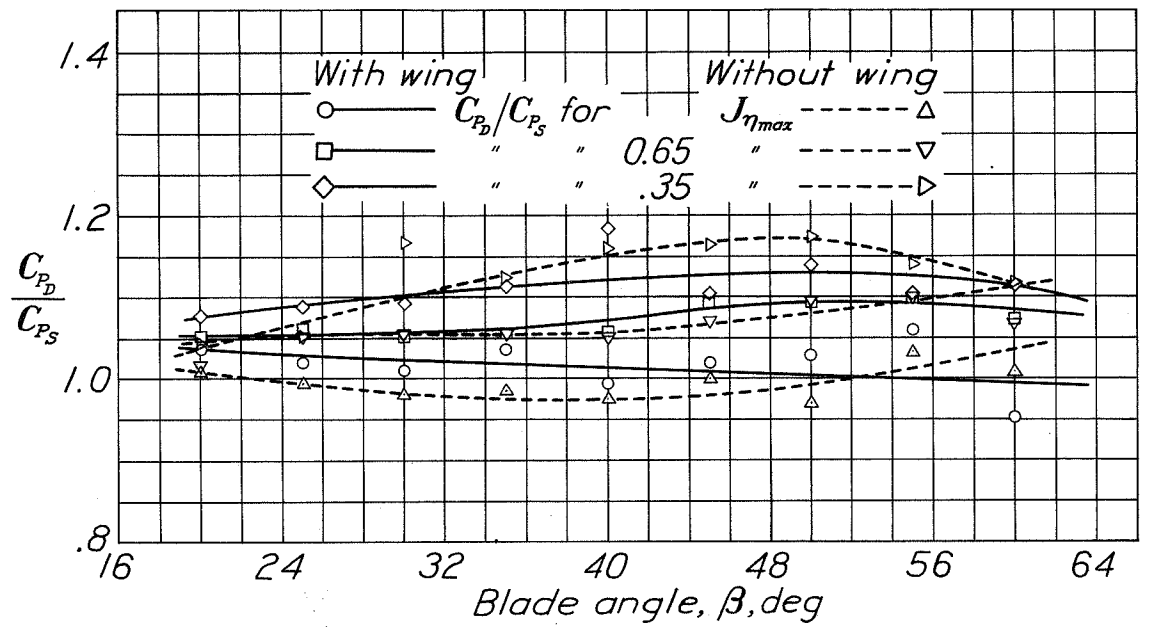

Figure 38.- Ratio of $\frac{C_P\text{- dual rotation}}{C_P\text{- single rotation}}$ in take-off, climb, and at peak efficiency for the four-blade propeller.

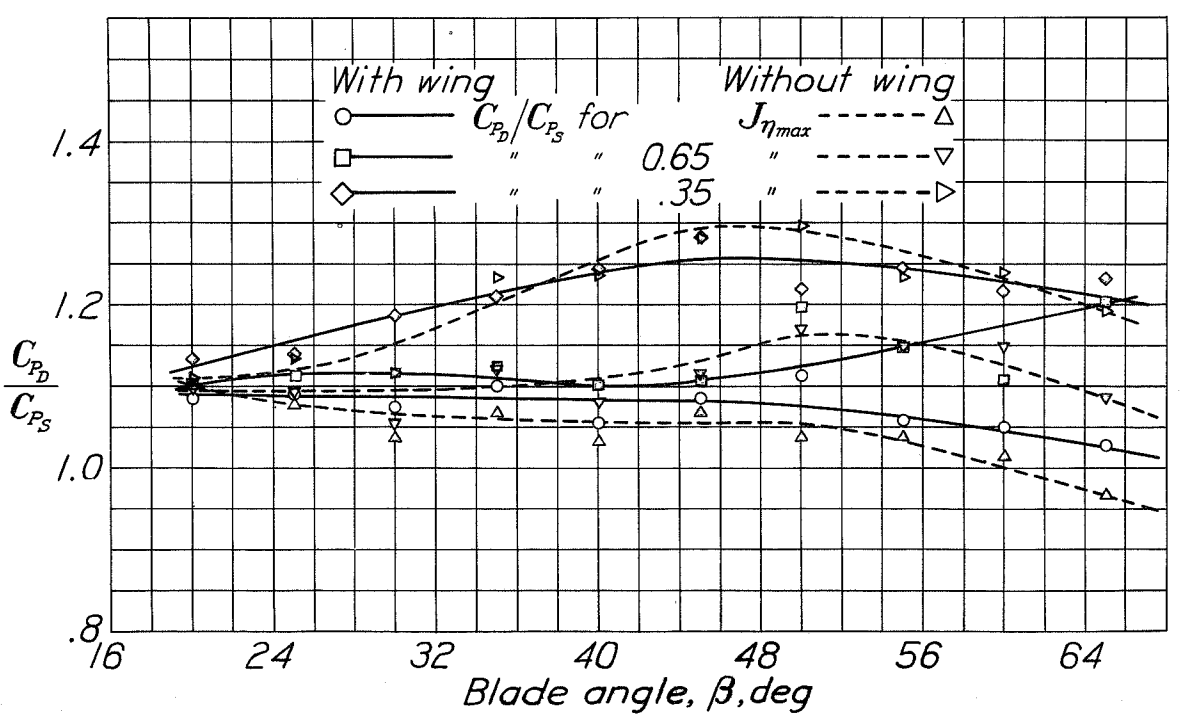

Figure 39.- Ratio of $\frac{C_P\text{-dual rotation}}{C_P\text{-single rotation}}$ in take-off, climb, and at peak efficiency for six-blade propeller.

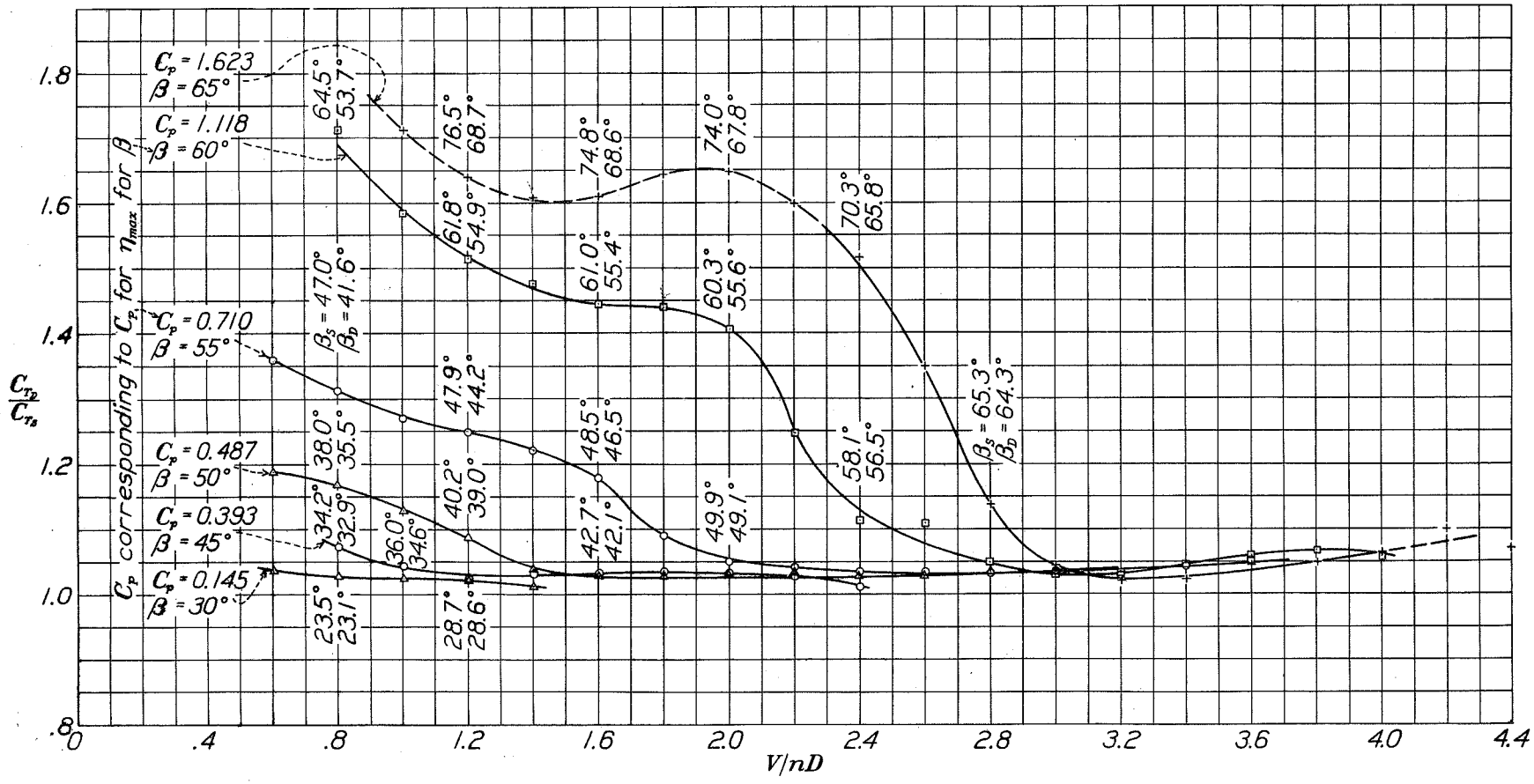

Figure 40.- Ratio of $\frac{C_T\text{-dual rotation}}{C_T\text{-single rotation}}$ for constant values of C_p. Six-blade propellers without wing.

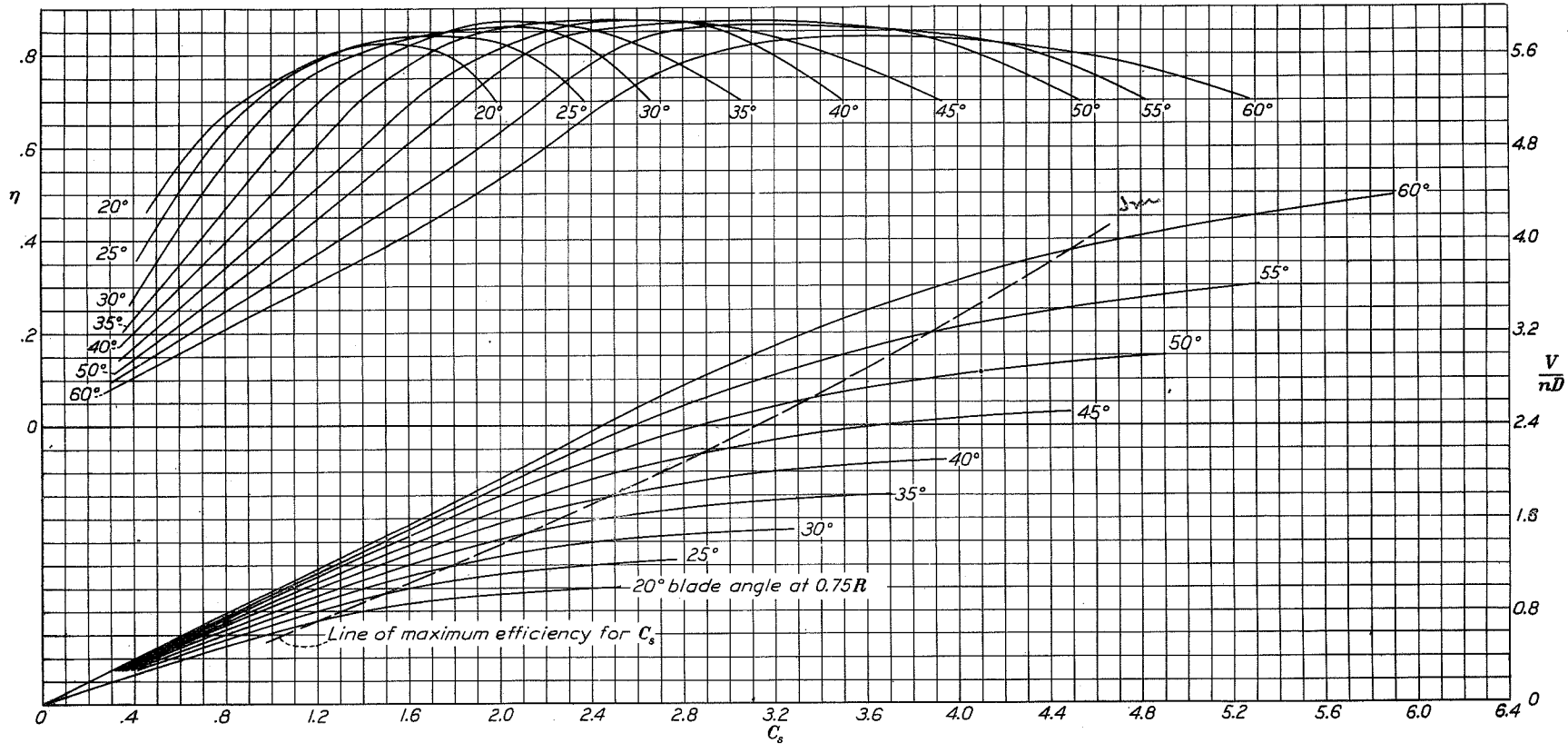

Figure 41.- Design chart for propellers 3155-6 and 3156-6, four-blade dual-rotation without wing.

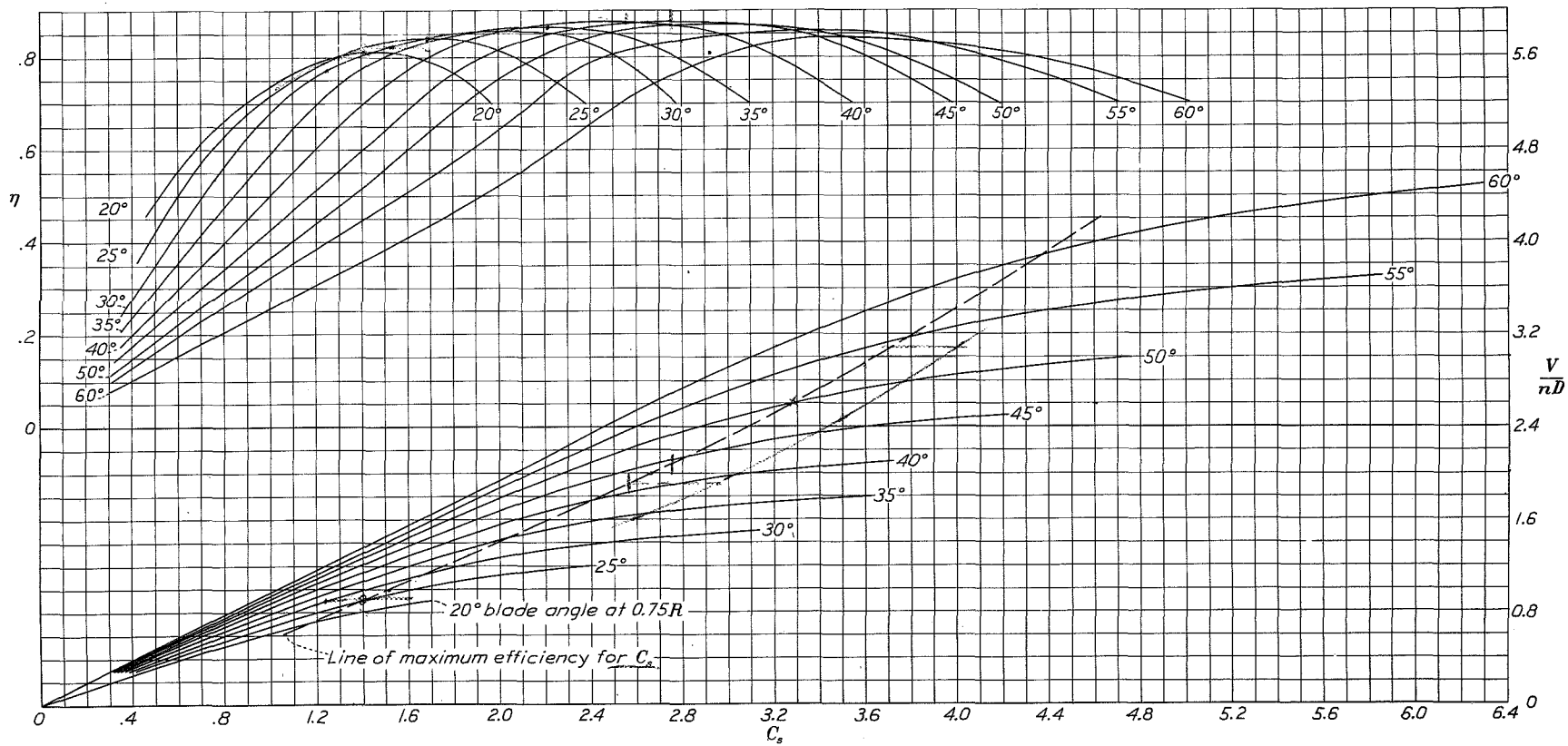

Figure 42.- Design chart for propellers 3155-6 and 3156-6, four-blade dual-rotation with wing

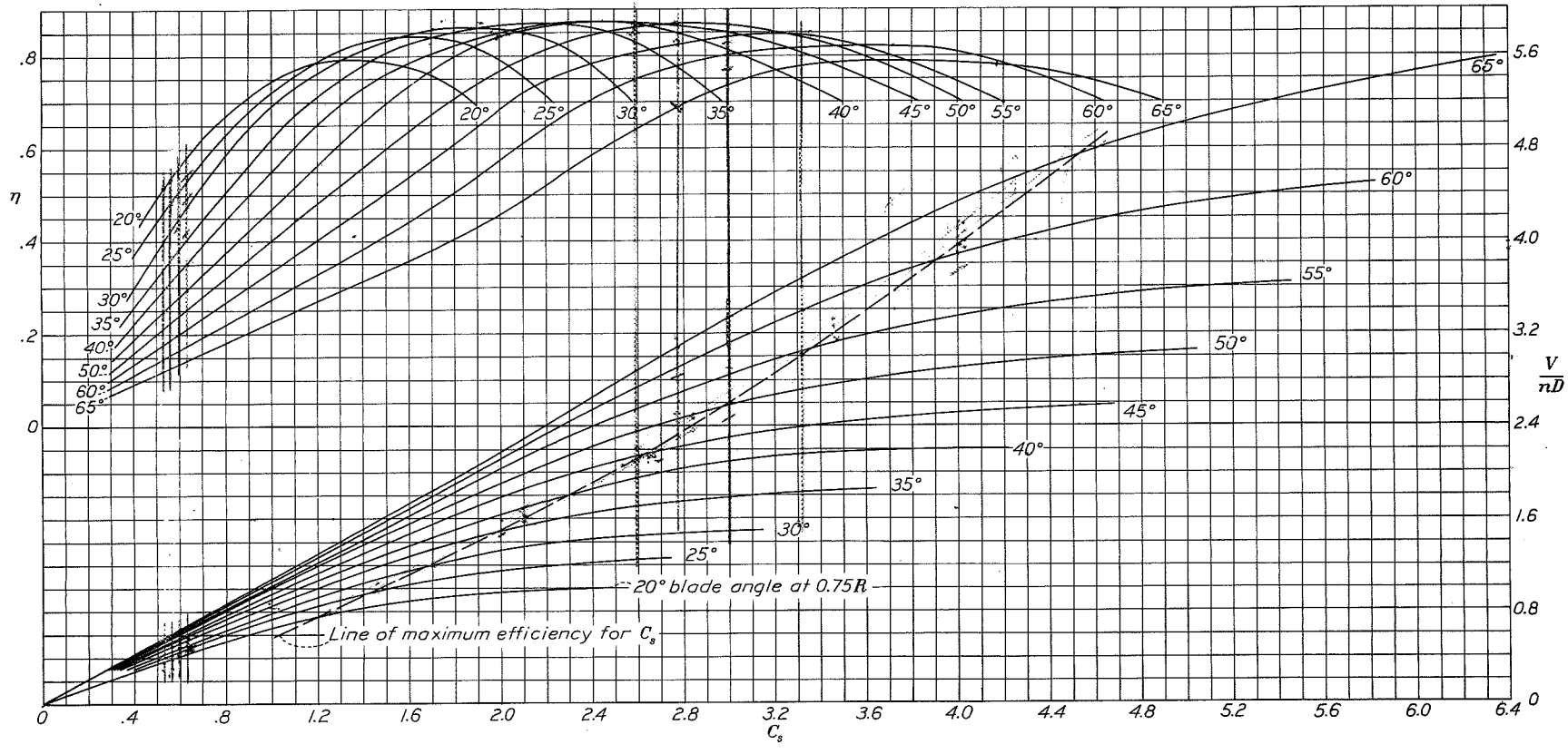

Figure 43.- Design chart for propellers 3155-6 and 3156-6, six-blade dual-rotation without wing.

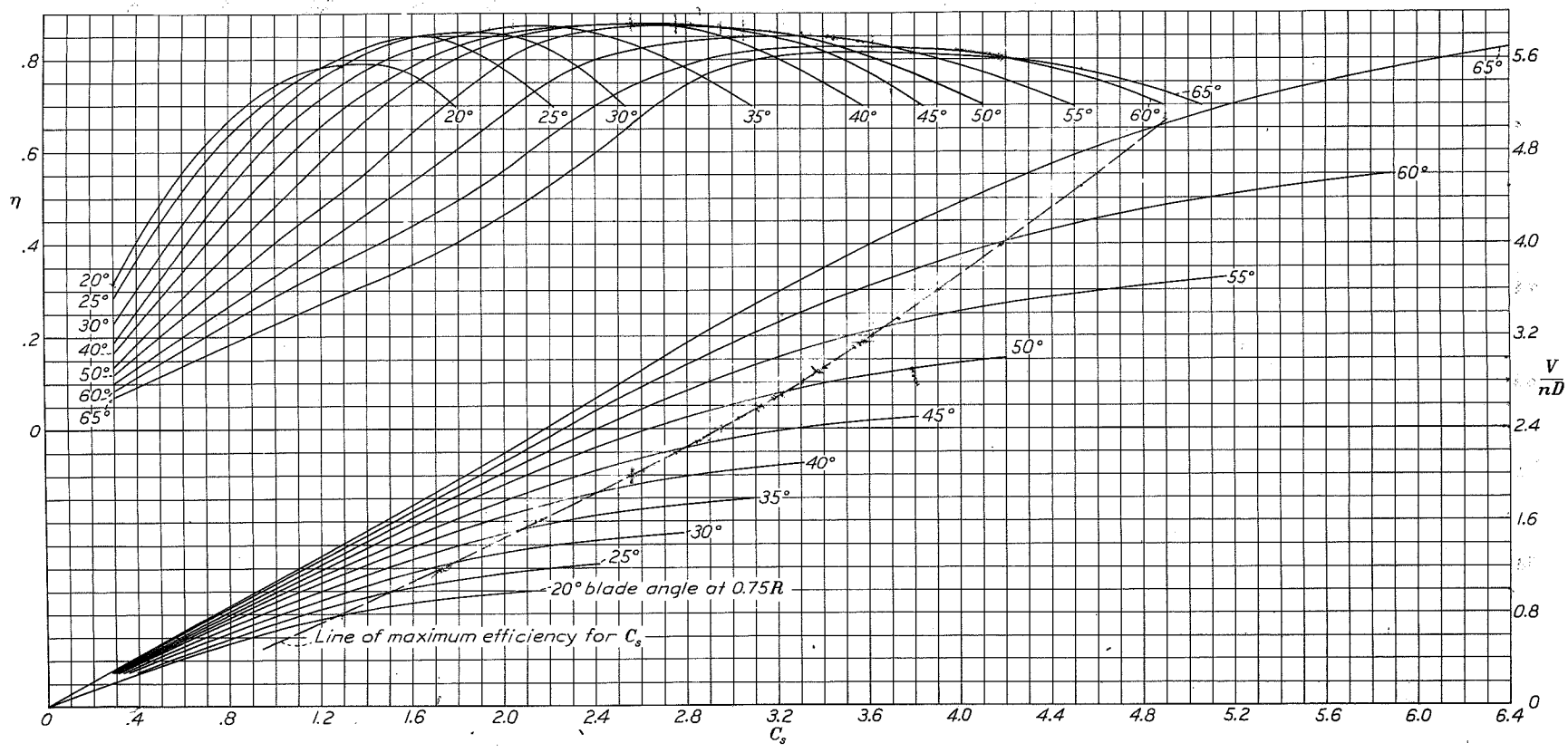

Figure 44.- Design chart for propellers 3155-6 and 3156-6, six-blade dual-rotation with wing.